nature immunology

Dectin-1 is required for host defense against *Pneumocystis carinii* but not against *Candida albicans*

Shinobu Saijo[1], Noriyuki Fujikado[1], Takahisa Furuta[2], Soo-hyun Chung[1], Hayato Kotaki[1], Keisuke Seki[1], Katsuko Sudo[1], Shizuo Akira[3], Yoshiyuki Adachi[4], Naohito Ohno[4], Takeshi Kinjo[5], Kiwamu Nakamura[5], Kazuyoshi Kawakami[6] & Yoichiro Iwakura[1]

Dectin-1 is a C-type lectin involved in the recognition of β-glucans found in the cell walls of fungi. We generated dectin-1-deficient mice to determine the importance of dectin-1 in the defense against pathogenic fungi. *In vitro*, β-glucan-induced cytokine production from wild-type dendritic cells and macrophages was abolished in cells homozygous for dectin-1 deficiency ('dectin-1-knockout' cells). *In vivo*, dectin-1-knockout mice were more susceptible than wild-type mice to pneumocystis infection, even though their cytokine production was normal. However, pneumocystis-infected dectin-1-knockout macrophages did show defective production of reactive oxygen species. In contrast to those results, wild-type and dectin-1-knockout mice were equally susceptible to candida infection. Thus, dectin-1 is required for immune responses to some fungal infections, as protective immunity to pneumocystis, but not to candida, required dectin-1 for the production of antifungal reactive oxygen species.

The C-type lectins form a group of proteins with a lectin-like carbohydrate-recognition domain in their extracellular carboxy-terminal domains[1]. Some C-type lectin family members recognize the carbohydrate structures of microbes as pathogen-associated molecular patterns, whereas other members, on natural killer cells, recognize endogenous ligands and discriminate self from nonself in a calcium-dependent way. Dectin-1 was first reported as a dendritic cell (DC)–specific type II C-type lectin receptor expressed as a 43-kilodalton membrane-associated glycoprotein, with a carbohydrate-recognition domain in its extracellular carboxyl terminus and an immunoreceptor tyrosine-based activation motif in its intracellular amino terminus[2,3]. Dectin-1 is also highly expressed on macrophages and neutrophils and is the receptor for β-1,3-linked and/or β-1,6-linked glucans (β-glucans)[4].

The β-glucans are important cell wall components of fungi and yeasts; they consist of a backbone of polymerized β(1→3)-linked β-D-glucopyranosyl units and β(1→6)–linked side chains[5] and are found in a wide-range of mushrooms, seaweeds, yeasts and pathogenic fungi. Although individual β-glucans are heterogeneous in terms of molecular weight, number of branches and helical construction, many β-glucans have immunological 'effector' activities *in vitro* and *in vivo*, and some are used beneficially to treat human diseases[6,7]. However, the mechanism of β-glucan-induced activity has not been elucidated completely because it has been difficult to discriminate the responses caused by β-glucans from those caused by other pathogen-derived components that are often contaminants of β-glucan preparations.

Studies have suggested that dectin-1 is involved in the recognition of and host defense mechanisms against pathogenic fungi, including *Candia albicans* and *Pneumocyctis carinii*, because those fungi express β-glucans in their cell walls and cause cytokine production after infection[8,9]. As for the defense mechanisms against fungi, both the innate and acquired immune systems are thought to be involved[10]. T helper 1 cell–mediated immune responses and the opsonization of fungi and their incorporation into macrophages through Fc receptors are important immune responses to fungal infection in immunocompetent people; that is reflected in the fact that fungal infection causes morbidity and mortality only in immunocompromised patients[10,11].

Cytokines induced by fungi are also important in activating immune responses and phagocytic cells. The many Toll-like receptors (TLRs) are thought to be critically involved in the cytokine responses to fungi because, for example, the survival of *Tlr2*$^{-/-}$ mice infected with *C. albicans* is much lower that of infected wild-type mice[12]; moreover, the cell walls of *C. albicans* can induce tumor necrosis factor (TNF) production by macrophages via TLR4 stimulation[13]. Although the mannose receptor (MRC1) has also been linked to the recognition

[1]Center for Experimental Medicine and [2]Department of Microbiology and Immunology, The Institute of Medical Science, The University of Tokyo, 4-6-1, Shirokanedai, Minato-ku, Tokyo 108-8639, Japan. [3]Department of Host Defense, Research Institute for Microbial Disease, Osaka University, 3-1 Yamadaoka, Suita-shi, Osaka 565-0871, Japan. [4]Laboratory for Immunopharmacology of Microbial Products, School of Pharmacy, Tokyo University of Pharmacy and Life Science, 1423-1 Horinouchi, Hachioji, Tokyo 192-0392, Japan. [5]Department of Medicine and Therapeutics, Control and Prevention of Infectious Diseases, Faculty of Medicine, University of the Ryukyu, 207 Uehara, Nishihara-cho, Nakagami-gunn, Okinawa 903-0215, Japan. [6]Microbiology and Immunology, Department of Medical Technology, School of Health Science, Tohoku University, 2-1, Seiryou-cho, Aoba-ku, Sendai-shi, Miyagi 980-8575, Japan. Correspondence should be addressed to Y.I. (iwakura@ims.u-tokyo.ac.jp).

Received 18 July; accepted 17 November; published online 10 December 2006; doi:10.1038/ni1425

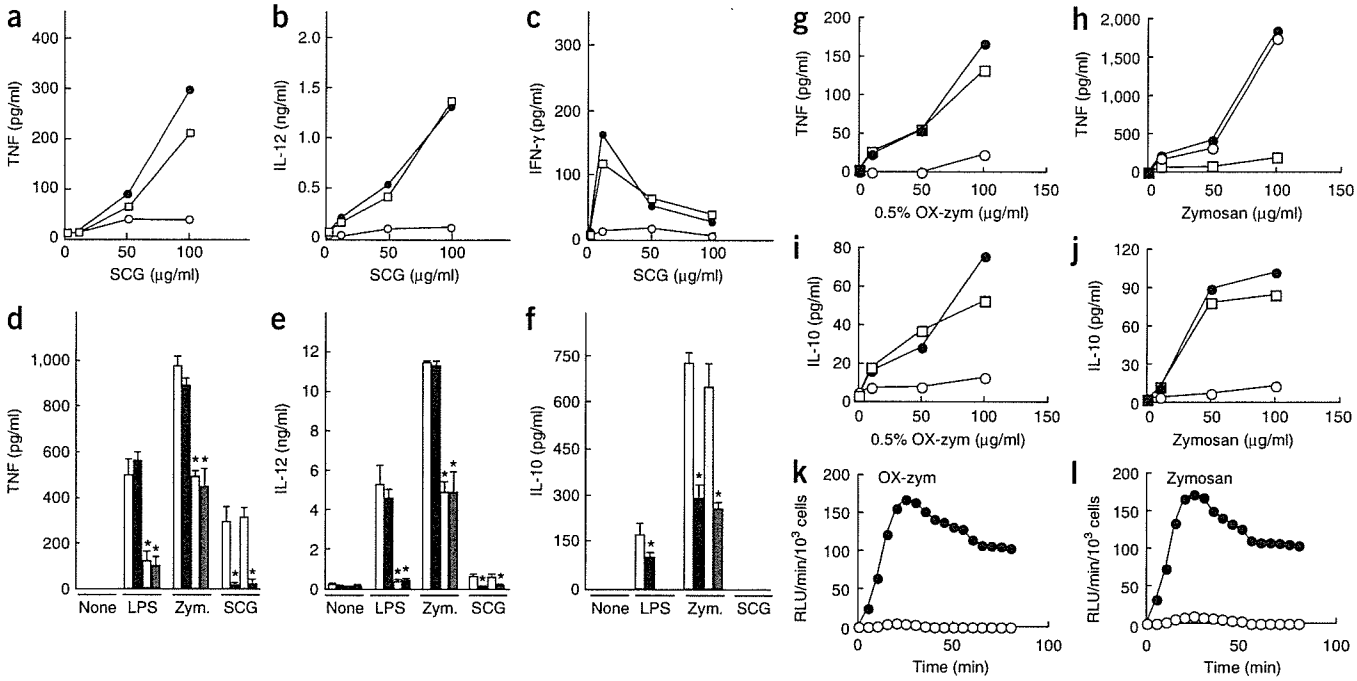

Figure 1 Cytokine induction by β-glucans is dependent on dectin-1. (**a–f**) ELISA of cytokine concentrations in supernatants of dectin-1-wild-type, dectin-1-knockout *Myd88*$^{+/+}$ and/or *Myd88*$^{-/-}$ BMDCs cultured for 24 h with SCG (**a–c**; concentration, horizontal axes) or with LPS (20 ng/ml), zymosan (Zym.; 100 μg/ml) or SCG (100 μg/ml; **d–f**). Filled circles and white bars, dectin-1-wild-type, *Myd88*$^{+/+}$; open circles and black bars, dectin-1-knockout, *Myd88*$^{+/+}$; open squares and light gray bars, dectin-1-wild-type, *Myd88*$^{-/-}$; dark gray bars, dectin-1-knockout, *Myd88*$^{-/-}$. *, $P < 0.01$ (Student's *t*-test). Data represent mean (+ s.d.) of triplicate samples (**d–f**) and were reproducible in three independent experiments (**a–f**). (**g–j**) ELISA of cytokine concentrations in supernatants of wild-type (filled circles), dectin-1-knockout (open circles) or *Myd88*$^{-/-}$ (open squares) thioglycollate-elicited macrophages cultured for 24 h with NaClO-oxidized zymosan (OX-zym) or zymosan (concentration, horizontal axes). (**k,l**) Luminol-enhanced chemiluminescence analysis of ROS produced by wild-type (filled circles) or dectin-1-knockout (open circles) thioglycollate-elicited macrophages stimulated with NaClO-oxidized zymosan (**k**) or zymosan (**l**). RLU, relative luciferase units. Similar results were obtained in one other independent experiment (**g–l**).

and phagocytosis of fungi via mannans expressed on fungal cell walls[14], *Mrc1*$^{-/-}$ mice show normal responses to *C. albicans* and *P. carinii* infection[15,16]. In addition to those host molecules, the importance of dectin-1 in recognizing and responding to fungal β-glucans *in vivo* remains to be fully elucidated. Here we describe the generation of mice homozygous for deficiency of the gene encoding dectin-1 (called 'dectin-1-knockout mice' here) and experiments done to assess the function of dectin-1 in host defense against fungal pathogens. Dectin-1 signaling activated DCs and macrophages to produce cytokines and reactive oxygen species (ROS), and dectin-1 was important in protection against *P. carinii* but not *C. albicans* infection.

RESULTS

Dectin-1-knockout mice develop normally

We generated embryonic stem cells heterozygous for dectin-1 deficiency by replacing both exon 1, containing the translation start site, and exon 2 of the gene encoding dectin-1 with a neomycin-resistance gene (**Supplementary Fig. 1** online). Dectin-1-knockout mice were born at the expected mendelian ratio, were fertile and showed no gross phenotypic abnormalities, including no alterations in lymphoid cell populations (data not shown). We did not detect dectin-1 mRNA in spleen cells from dectin-1-knockout mice (**Supplementary Fig. 1**), and there was no dectin-1 expression on the surfaces of dectin-1-knockout bone marrow–derived DCs (BMDCs; **Supplementary Fig. 1**), indicating that the gene encoding dectin-1 was correctly disrupted.

Dectin-1 is required for β-glucan activation of DCs

As dectin-1 is considered a receptor for β-glucans, we examined the responses of wild-type and dectin-1-knockout BMDCs to β-glucans. We used *Sparassis crispa* glucan (SCG), a soluble, β-1,6-branched β-1,3-glucan purified from the edible mushroom, because it is biologically active and is easily purified to homogeneity[17]. After stimulation of wild-type BMDCs with SCG, production of interleukin 12 (IL-12) and TNF was enhanced in a dose-dependent way (**Fig. 1a,b**). Production of interferon-γ (IFN-γ) was also stimulated by SCG, although production was suppressed at higher concentrations (**Fig. 1c**). In contrast, production of those cytokines was completely abolished in dectin-1-knockout BMDCs (**Fig. 1a–c**), indicating that dectin-1 is required for cytokine induction in BMDCs after β-glucan stimulation.

Zymosan, a polysaccharide particle from the cell wall of *Saccharomyces cerevisiae*, is one of most commonly used β-glucan-containing experimental agents, although it contains other components, including mannans, other glucans and chitins[18]. Studies have suggested that the induction of TNF and IL-12 in response to zymosan requires the 'collaboration' of dectin-1 and TLR2 (ref. 19) on the cell surface, followed by activation of the transcription factor NF-κB via MyD88 (refs. 20,21), an intracellular signal transducer required for TLR signaling[22]. To determine the relative requirements for dectin-1 and MyD88 in BMDC responses to zymosan and SCG and to the MyD88-dependent stimulus lipopolysaccharide (LPS), we assessed cytokine production in BMDCs from dectin-1-knockout and *Myd88*$^{-/-}$ mice. Cytokine production induced by LPS was completely

dependent on MyD88 (**Figs. 1d–f**), as reported before[23]. In contrast, the SCG-induced production of TNF, IL-12 and IFN-γ was not affected at all by the lack of MyD88 (**Figs. 1a–f**). After stimulation with zymosan, in contrast, production of TNF and IL-12 was significantly reduced in *Myd88*$^{-/-}$ BMDCs but not in dectin-1-knockout BMDCs. Production of those cytokines, therefore, was dependent on TLR but not dectin-1 signaling. We also found that IL-10 production stimulated by zymosan was suppressed in dectin-1-knockout BMDCs but not in *Myd88*$^{-/-}$ BMDCs, suggesting that the induction mechanisms for IL-10 versus those for IL-12 and TNF are distinct (**Fig. 1f**). Zymosan-induced TNF and IL-12 production in dectin-1-knockout and *Myd88*$^{-/-}$ double-deficient BMDCs did not differ significantly from that in *Myd88*$^{-/-}$ single-deficient BMDCs (**Fig. 1d,e**), and IL-10 production was similar to that of dectin-1-knockout BMDCs (**Fig. 1f**). These results indicated that cytokine production via dectin-1 signaling is independent of MyD88 and that zymosan stimulates both dectin-1 and MyD88.

To further discriminate molecules that activate dectin-1 from those that activate MyD88, we compared the cytokine-stimulatory effect of NaClO-oxidized zymosan versus that of untreated zymosan on thioglycollate-elicited macrophages. The nitrogen content of zymosan is 1.81%, and it becomes 0.18% after treatment with 0.5% NaClO and 0.1 M NaOH; treating zymosan in that way results in a product composed mainly of β-glucans[24]. We found that although TNF was induced in both wild-type and *Myd88*$^{-/-}$ thioglycollate-elicited macrophages by NaClO-oxidized zymosan in a dose-dependent way, production of TNF was abolished in dectin-1-knockout thioglycollate-elicited macrophages (**Fig. 1g**). In contrast, production of TNF was not affected in dectin-1-knockout thioglycollate-elicited macrophages treated with intact zymosan, whereas it was reduced in *Myd88*$^{-/-}$ macrophages (**Fig. 1h**). Finally, we found that IL-10 induction was completely dependent on dectin-1 but not on MyD88, as with BMDCs (**Fig. 1i,j**). We next examined production of ROS, which is important for killing microbes that are phagocytosed by macrophages[25]. We found that production of ROS by thioglycollate-elicited macrophages was completely depended on dectin-1 for both zymosan and NaClO-oxidized zymosan (**Fig. 1k,l**). Our data collectively indicated that production of IL-10 and ROS is completely dependent on dectin-1, whereas TNF production by thioglycollate-elicited macrophages after zymosan treatment is mediated by molecules other than β-glucans that stimulate the MyD88 signaling pathway.

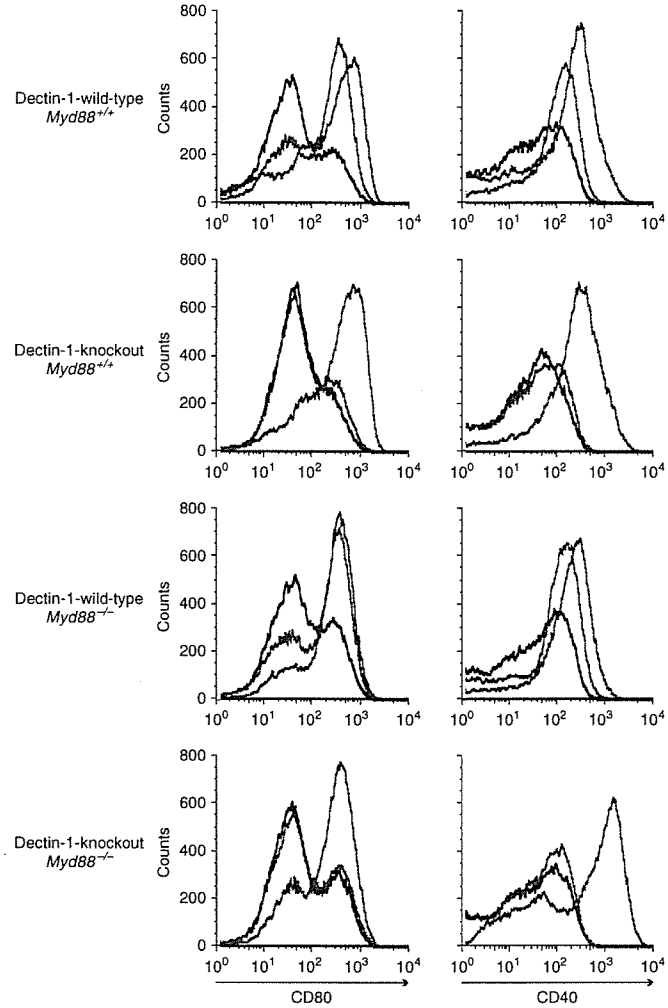

Figure 2 BMDC maturation is induced by β-glucans via dectin-1. Flow cytometry of the expression of CD80 and CD40 on CD11c$^+$ BMDCs cultured for 24 h with SCG (100 μg/ml; red lines) or LPS (20 ng/ml; blue lines) or without any stimulation (black lines). Data are representative of three independent experiments.

Dectin-1 signaling induces the SCG maturation of BMDCs

As stimulation by β-glucans has been suggested to be involved in the maturation of BMDCs[26], we next examined the cell surface expression of CD80 and CD40, maturation markers of DCs, after treatment of BMDCs with SCG. Immature BMDCs incubated for 24 h with SCG showed enhanced expression of both CD80 and CD40 (**Fig. 2**). However, there was no enhancement in dectin-1-knockout BMDCs, suggesting that dectin-1 is critical for SCG-inducted activation of BMDCs. To determine if the dectin-1-knockout BMDCs had an intrinsic 'maturation defect', we also treated them separately with LPS, which was sufficient to cause full maturation (at least by the criteria we used). In contrast to the results obtained with dectin-1-knockout BMDCs, *Myd88*$^{-/-}$ BMDCs matured normally after stimulation with SCG, indicating again that activation of BMDCs via dectin-1 is independent of the MyD88 pathway.

T cell–mediated responses are normal in dectin-1-knockout mice

It has been reported that soluble recombinant dectin-1 can bind to the surfaces of T cells and promote proliferation induced by antibody to CD3 (anti-CD3), suggesting the presence of an unknown endogenous dectin-1 ligand on T cells[2]. To evaluate that phenomenon in cells lacking dectin-1 expression, we next assayed proliferation. CD4$^+$ T cells cultured with dectin-1-knockout DCs and monoclonal anti-CD3 had proliferative activity equal to that of wild-type DCs (**Fig. 3a**). Also, the antigen-presenting activity of ovalbumin peptide–loaded dectin-1-knockout DCs to DO11.10-transgenic CD4$^+$ T cells was indistinguishable from the activity of wild-type DCs (**Fig. 3b**). Furthermore, production of antibodies to sheep red blood cells or to dinitrophenol–keyhole limpet hemocyanin was normal in dectin-1-knockout mice (**Fig. 3c** and data not shown), and delayed-type hypersensitivity responses to methylated bovine serum albumin were normal in dectin-1-knockout mice (**Fig. 3d**). These results indicated that a possible costimulatory effect of dectin-1 on T cell proliferation by means of T cell–expressed endogenous ligands (if they exist) is not essential.

Protection against *P. carinii* infection requires dectin-1

Because β-glucan, in addition to mannose-containing polysaccharides[27], is a chief cell wall component of *P. carinii*, we examined

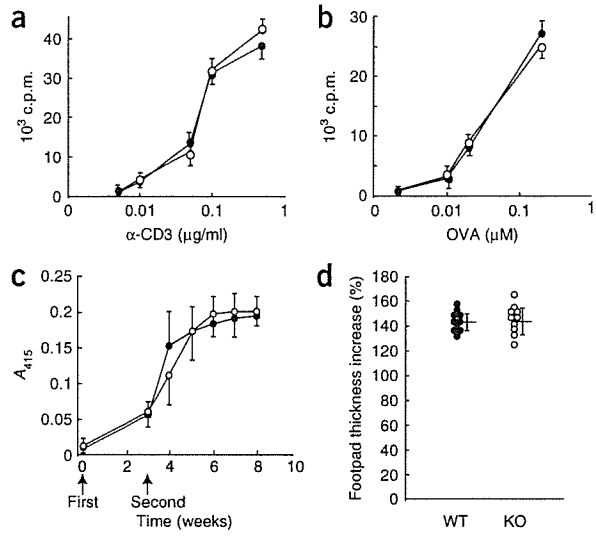

Figure 3 Antigen presentation by dectin-1-knockout dendritic cells is normal. (**a**) Proliferation assay of wild-type $CD4^+$ T cells cultured for 3 d with $CD11c^+$ DCs from BALB/c dectin-1-wild-type or dectin-1-knockout mice in the presence of anti-CD3 before analysis of [^{3}H]thymidine incorporation. (**b**) Antigen-presenting activity of DCs, assessed as proliferation of $CD4^+$ T cells from DO11.10-transgenic mice, cultured for 3 d with $CD11c^+$ DCs from BALB/c dectin-1-wild-type or dectin-1-knockout mice in the presence of ovalbumin peptide (OVA) before analysis of [^{3}H]thymidine incorporation. Filled circles, dectin-1-wild-type; open circles, dectin-1-knockout. Data are mean (+ s.d.) of triplicate samples and are representative of three independent experiments (**a**,**b**). (**c**) ELISA of the production of antibodies to sheep red blood cells by dectin-1-wild-type and dectin-1-knockout mice at 21 d after secondary immunization, assessed as alkaline phosphatase activity (mean + s.d.). Upward arrows, first (left) and second (right) immunization. A_{415}, absorbance at 415 nm. Data are representative of one experiment. (**d**) Delayed-type hypersensitivity responses in dectin-1-wild-type mice (WT) and dectin-1-knockout mice (KO), assessed as increase in footpad thickness induced by methylated bovine serum albumin. Each circle represents an individual mouse; data represent mean (+ s.d.) for one experiment. Filled circles, dectin-1-wild-type (n = 10 mice in each); open circles, dectin-1-knockout (n = 10 mice in each).

the susceptibility of dectin-1-knockout mice to *P. carinii*. Dectin-1-knockout mice inoculated with 1.7×10^4 *P. carinii* cysts had many more organisms at 1 or 2 weeks after infection than did similarly infected wild-type mice, indicating that dectin-1-knockout mice are more sensitive (**Fig. 4a**). In contrast to those results early after infection, we did not detect *P. carinii* in either wild-type or dectin-1-knockout mice either 20 d or 4 months after infection (less than 1.5×10^2 cysts per mouse). We also infected nude mice, which lack T cells, in the same way and detected $2.6 \times 10^5 \pm 3.8 \times 10^5$ cysts in their lungs 4 months after infection, which indicated a critical function for T cell–mediated immune responses in the host defense against *P. carinii*. Thus, in the presence of an intact acquired immune system, dectin-1 is not required for protection against chronic infection by *P. carinii*.

As another means of assessing the importance of dectin-1 early after infection with *P. carinii*, we examined the susceptibility of immunocompromised but otherwise normal wild-type and dectin-1-knockout mice. We gave the mice cortisone acetate twice weekly (2.5 mg/mouse), then infected them intranasally with *P. carinii* (6.4×10^5 cysts per mouse) and counted cysts in the lungs 24 d later. Wild-type and dectin-1-knockout mice were equally sensitive to cortisone treatment, as the number of the white blood cells before and after treatment with cortisone was similar for those two strains (before treatment: wild-type, 11,700 ± 1,600 cells/μl, and dectin-1-knockout, 11,600 ± 1,600 cells/μl; after treatment: wild-type, 780 ± 580 cells/μl, and dectin-1-knockout, 880 ± 440 cells/μl). However, even though the two strains of mice were equally immunocompromised, dectin-1-knockout mice had significantly more cysts in their lungs ($2.5 \times 10^5 \pm 0.78 \times 10^5$ cysts per mouse) than wild-type mice did ($5.6 \times 10^4 \pm 4.2 \times 10^4$ cysts per mouse; **Fig. 4b**). These observations demonstrated that dectin-1 is important in host defense mechanisms against *P. carinii*.

P. carinii–induced ROS require dectin-1

Because TNF, IFN-γ and IL-12 are higher in *P. carinii*–infected mice[28] and because TNF and IFN-γ are reported to be important in protection against *P. carinii*[29], we measured cytokine production in dectin-1-knockout macrophages cultured with *P. carinii* cysts *in vitro*.

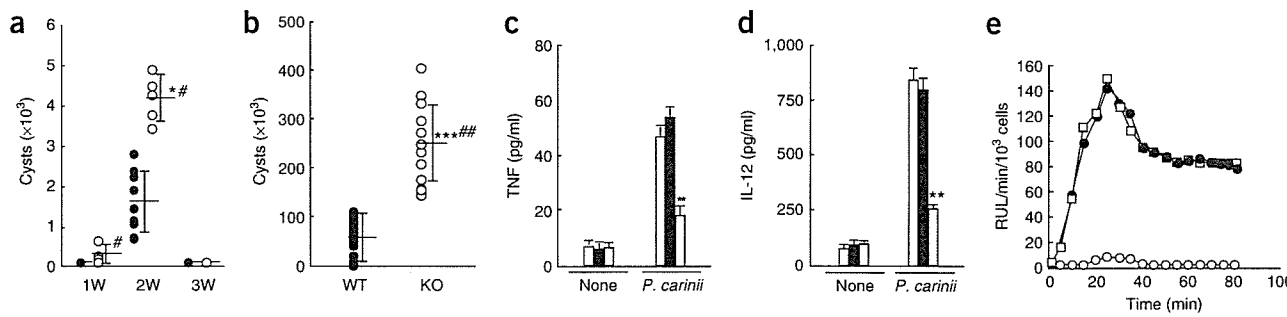

Figure 4 Dectin-1-knockout mice are more susceptible than dectin-1-wild-type mice to *P. carinii* infection. (**a**) *P. carinii* cysts in the lungs of dectin-1-wild-type mice (filled circles) and dectin-1-knockout mice (open circles) inoculated intranasally with 1.7×10^4 *P. carinii* cysts for 1 week (1W; wild-type, n = 7; knockout, n = 4), 2 weeks (2W; wild-type, n = 9; knockout, n = 5) or 3 weeks (3W; wild-type, n = 5; knockout, n = 5), determined by counting of toluidine blue O–positive cells. (**b**) *P. carinii* cysts in the lungs of dectin-1-wild-type mice (WT; n = 21) and dectin-1-knockout mice (KO; n = 14) inoculated intranasally with 6.4×10^5 *P. carinii* cysts and given 2.5 mg cortisone acetate per mouse twice weekly, determined 24 d after inoculation by counting of toluidine blue O–positive cells. *, $P < 0.05$, and ***, $P < 0.001$ (Mann-Whitney U test); #, $P < 0.05$, and ##, $P < 0.01$ (Student's t-test). Each circle represents an individual mouse (**a**,**b**); data represent mean (+ s.d.) and are from one experiment (**a**) or were reproduced in four independent experiments (**b**). (**c**,**d**) ELISA of TNF (**c**) or IL-12 (**d**) in supernatants from dectin-1-wild-type (white bars), dectin-1-knockout (black bars) or *Myd88*$^{-/-}$ (gray bars) alveolar macrophages (pooled from three mice) cultured for 24 h with (right) or without (left; None) *P. carinii* cysts. **, $P < 0.01$ (Student's t-test). Data represent mean (+ s.d.) from three wells and were reproduced in at least three independent experiments. (**e**) Luminol-enhanced chemiluminescence analysis of ROS produced by wild-type (filled circles), dectin-1-knockout (open circles) or *Myd88*$^{-/-}$ (open squares) alveolar macrophages. Data were reproducible in three independent experiments.

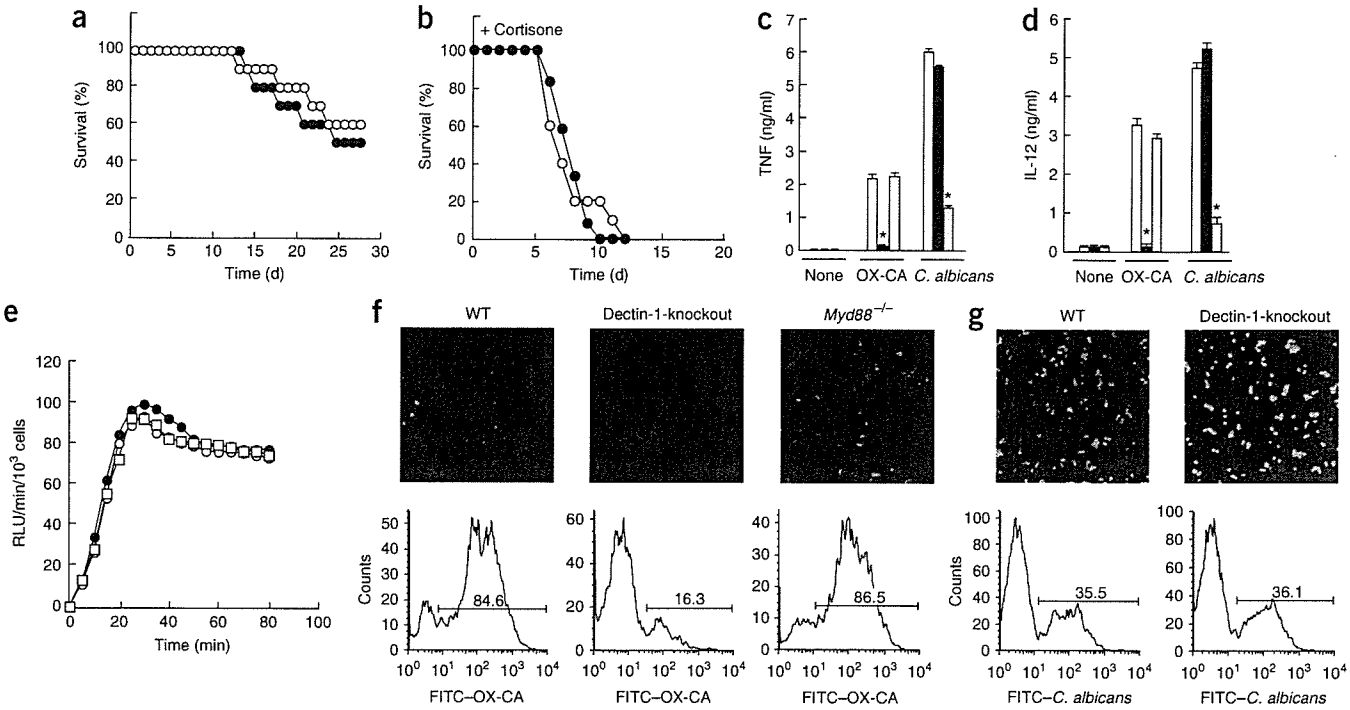

Figure 5 Dectin-1 is not required for defense against *C. albicans*. (**a**) Survival of dectin-1-wild-type mice ($n = 10$; filled circles) and dectin-1-knockout mice ($n = 10$; open circles) on a C57BL/6J background, infected intravenously with 2×10^5 *C. albicans*. (**b**) Survival of dectin-1-wild-type mice ($n = 12$; filled circles) and dectin-1-knockout mice ($n = 10$; open circles) on a BALB/cA background in an immunocompromised condition (+ Cortisone), after infection with 2×10^5 *C. albicans*. (**c**,**d**) ELISA of cytokines in supernatants of dectin-1-wild-type (white bars), dectin-1-knockout (black bars) and *Myd88*$^{-/-}$ (gray bars) alveolar macrophages (C57BL/6J background) cultured for 24 h with NaClO-oxidized candida (OX-CA; 100 μg/ml) or *C. albicans* (multiplicity of infection, 10). Data represent mean (+ s.d.) of triplicate samples and were reproduced in three independent experiments. (**e**) ROS in supernatants of alveolar macrophages from dectin-1-wild-type (filled circles), dectin-1-knockout (open circles) or *Myd88*$^{-/-}$ (open squares) C57BL/6J mice; cells (pooled from three mice) were stimulated with *C. albicans*. *, $P < 0.01$ (Student's *t*-test). Data were reproducible in three independent experiments. (**f**,**g**) Confocal laser microscopy (top rows) and flow cytometry (bottom rows) of thioglycollate-elicited dectin-1-wild-type (WT), dectin-1-knockout and *Myd88*$^{-/-}$ macrophages cultured for 60 min together with FITC-labeled NaClO-oxidized candida (100 μg/ml; **f**) or with FITC-labeled *C. albicans* (1×10^5 cells; **g**). For microscopy, coculture (FITC, green) was followed by macrophage staining with CM-DiI (red). For flow cytometry, coculture was followed by staining with phycoerythrin-conjugated anti–mouse CD11b (**f**) or with CM-DiI (**g**); numbers above bracketed lines indicate percent FITC$^+$ cells in the CD11b$^+$ or DiI$^+$ cell population. Data are from one of two independent experiments (**f**,**g**).

Although production of TNF and IL-12 was not inhibited in dectin-1-knockout macrophages (**Fig. 4c,d**), cytokine production was much lower in *Myd88*$^{-/-}$ macrophages, indicating that cytokine induction by *P. carinii* is dependent on MyD88 signaling. In these conditions, we could not detect IL-10 production (data not shown). We also evaluated production of ROS. Although wild-type macrophages produced ROS after incubation with *P. carinii*, production of ROS was completely abolished in dectin-1-knockout macrophages incubated with *P. carinii* (**Fig. 4e**), indicating that dectin-1-induced signaling is essential for induction of ROS. In contrast, production of ROS in *Myd88*$^{-/-}$ macrophages was similar to that in wild-type macrophages (**Fig. 4e**), indicating that MyD88 signaling is not required for *P. carinii*–induced production of ROS. Thus, dectin-1 is crucial for the induction of ROS but not of TNF or IL-12 after infection with *P. carinii*.

Dectin-1-knockout mice are not more susceptible to *C. albicans*

To assess the effect of dectin-1 deficiency on systemic candidiasis, we infected mice intravenously with 2×10^5 *C. albicans* cells per mouse and then monitored the survival of the mice. Unexpectedly, we detected no difference in the survival of dectin-1-knockout and wild-type mice (**Fig. 5a**), even after several doses of *C. albicans* (2×10^4, 1×10^5, 5×10^5 or 1×10^6 fungi per mouse all resulted in similar survival; **Supplementary Fig. 2** online and data not shown). We also did not detect significant differences in fungal burdens in the lungs of dectin-1-knockout and wild-type mice after intratracheal administration of *C. albicans* (**Supplementary Fig. 2**). We also examined the sensitivity of dectin-1-knockout mice to *C. albicans* infection in immunocompromised conditions. When we treated mice with cortisone and infected them intravenously with 2×10^5 *C. albicans*, there was no significant difference in the survival rates of dectin-1-knockout mice and wild-type mice (**Fig. 5b**). Thus, in contrast to the results we obtained after infection with *P. carinii*, dectin-1 is dispensable for the host defense against *C. albicans*.

C. albicans–induced ROS and cytokines do not require dectin-1

We next examined cytokine production in dectin-1-knockout macrophages after treatment with a β-glucan preparation purified from *C. albicans* or with live fungal cells. Although there was significant induction of TNF and IL-12 in wild-type macrophages stimulated with NaClO-oxidized candida, a particle-form β-1,6-branched β-1,3-glucan derived from *C. albicans*, production of those cytokines was completely abolished in dectin-1-knockout macrophages (**Fig. 5c,d**). In contrast, cytokine production was not reduced in dectin-1-knockout macrophages cultured with live *C. albicans*. Also, TNF and IL-12 production was not lower in *Myd88*$^{-/-}$ macrophages

than in wild-type macrophages after induction with NaClO-oxidized candida, but it was significantly lower in *Myd88*$^{-/-}$ macrophages after infection with *C. albicans*, indicating that β-glucans are not the main inducer of cytokines after infection. In addition, production of ROS by dectin-1-knockout macrophages after infection with *C. albicans* was similar to that of wild-type macrophages, indicating that in contrast again to its function during *P. carinii* infection, dectin-1 is not required for *C. albicans*–induced production of ROS (**Fig. 5e**). MyD88 was also not involved in the induction of ROS by *C. albicans*.

Finally, we found that dectin-1-knockout macrophages did not bind NaClO-oxidized candida, whereas wild-type or *Myd88*$^{-/-}$ macrophages did efficiently bind that form of β-glucan (**Fig. 5f**). In contrast, dectin-1-knockout macrophages bound untreated *C. albicans* as efficiently as wild-type macrophages did (**Fig. 5g**), indicating that molecules other than β-glucan are required. These results indicated that dectin-1 is the only receptor for the β-1,3- and β-1,6-glucans derived from *C. albicans*, whereas other molecules are mainly involved in the induction of cytokines and ROS after infection of this fungus.

DISCUSSION

Here we have provided definitive evidence that dectin-1 is the sole receptor for β-glucans, that dectin-1 is required for production of cytokines and ROS from both DCs and macrophages after stimulation with β-glucans, that dectin-1 is required for DC maturation induced by SCG and that dectin-1 is required for optimal host defense against *P. carinii* but not *C. albicans*. We have demonstrated that TNF and IL-12 production was abolished in dectin-1-knockout BMDCs, alveolar macrophages and thioglycollate-elicited macrophages after stimulation with purified β-glucans such as SCG, NaClO-oxidized zymosan or NaClO-oxidized candida. *Myd88*$^{-/-}$ and wild-type BMDCs, in contrast, produced similar amounts of cytokines, indicating that MyD88 is not involved in dectin-1 signaling. We also found that dectin-1-knockout BMDCs and thioglycollate-elicited macrophages treated with zymosan produced normal amounts of TNF, whereas *Myd88*$^{-/-}$ cells produced much less, suggesting that zymosan-induced cytokine production is dependent on TLRs.

TNF production in BMDCs induced by either *P. carinii* or *C. albicans* was also unaffected by dectin-1 deficiency, although it was lower in *Myd88*$^{-/-}$ cells. Those observations are consistent with a published report that TLR2 and TLR6 signaling are important in zymosan-induced cytokine production in a macrophage cell line (RAW cells)[22]. However, we did find that zymosan-induced IL-10 production was much lower in dectin-1-knockout BMDCs and thioglycollate-elicited macrophages, which was consistent with a report that DCs deficient in Syk, a protein kinase 'downstream' of dectin-1, do not produce any IL-10 but instead produce IL-12 after stimulation with zymosan[30]. We also found that the binding of NaClO-oxidized candida to dectin-1-knockout thioglycollate-elicited macrophages was much lower than its binding to wild-type cells, whereas the binding of untreated *C. albicans* cells was not. Thus, living *P. carinii* and *C. albicans* induce cytokines, except IL-10, in a dectin-1-independent way, although those organisms express β-glucans that can activate dectin-1.

As only nude mice or cortisone-treated, immunocompromised wild-type mice are susceptible to *P. carinii*, it has been suggested that acquired immune responses are important mainly in the host defense mechanism. Our data that dectin-1-knockout mice were more susceptible than wild-type mice to *P. carinii* demonstrated that dectin-1 is required for defense against that pathogen. Because the production of cytokines such as IL-12 and TNF by dectin-1-knockout macrophages was similar to that of wild-type macrophages after infection with *P. carinii*, those cytokines, which are required for T helper 1 cell induction and B cell activation, may not function in protection against that organism.

Notably, we found that production of ROS was completely abolished in dectin-1-knockout mice after infection with *P. carinii*, indicating that production of ROS is entirely dependent on β-glucan–dectin-1 signaling. Zymosan-induced production of ROS in thioglycollate-elicited macrophages was also completely dependent on dectin-1, consistent with a published study[20]. Those results contrast with results demonstrating that production of TNF and IL-12 is induced more efficiently through TLRs. ROS, which are produced by macrophages after microbe infection, are thought to be important in antifungal protection[25], because ROS modify fungal proteins, break nucleic acids and oxidize lipid components[31]. Our observations here suggested that dectin-1 is important in the host defense against *P. carinii* by inducing ROS-mediated killing of the organism.

Although possible involvement of dectin-1 in T cell activation has been suggested[2], we have shown here that dectin-1 is not involved in anti-CD3-induced T cell proliferation, antigen presentation of DCs, production of antibodies to sheep red blood cells and to dinitrophenol–keyhole limpet hemocyanin, or the delayed-type hypersensitivity reaction. Moreover, we have shown that the protective effect of dectin-1 against *P. carinii* was present in immunocompromised conditions. Therefore, it is unlikely that dectin-1 is involved in the host defense against *P. carinii* through activation of T cell–dependent immunity.

In contrast to the results obtained with *P. carnii*, we found no significant difference in the survival and fungal loads of wild-type and dectin-1-knockout mice after infection with *C. albicans* in either immunocompetent or immunocompromised conditions. We found that β-glucans on *C. albicans* did not significantly contribute to macrophage production of cytokines after infection with *C. albicans*, although dectin-1-knockout macrophages failed to produce cytokines in response to NaClO-oxidized candida purified from *C. albicans*. Those results suggest that β-glucans on live fungal surfaces are not efficiently accessible to dectin-1, which has been indicated in a published study[9]. Instead, we found that MyD88-dependent signaling induced cytokines after candida infection, which is consistent with published reports[10,12,13]. There was similar production of ROS in alveolar macrophages from dectin-1-knockout and wild-type mice after infection with *C. albicans*. That result contrasts with those obtained after *P. carinii* or zymosan treatment of dectin-1-knockout cells showing that production of ROS was completely dependent on the presence of dectin-1.

After *C. albicans* infection, production of ROS was also normal in *Myd88*$^{-/-}$ macrophages. Thus, other molecules in the cell walls of *C. albicans* might stimulate host cells in the absence of the binding of β-glucan to dectin-1. *C. albicans* indeed has a multilayered cell wall composed of an outer layer containing *N*- and *O*-linked mannosyl residues and an inner skeletal layer of β-glucans and chitins[32], and it has been reported that host cell recognition of *C. albicans* is mediated by three different receptor systems (MR, TLR4 and a dectin-1–TLR2 hetero-receptor complex) and that β-glucans contribute only marginally to cytokine production[32]. The structure of fungal cell walls and the accessibility of β-glucans, TLR ligands and mannans in the cell walls to their cognate receptors may be different for different pathogens. Therefore, different combinations of host receptors are probably needed for host defense mechanisms against different fungi. In conclusion, our results suggest the importance of dectin-1 for protection against *P. carinii* and indicate dectin-1 is a 'second' defense mechanism, in addition to TLRs, required particularly in the absence of acquired immune responses. Such a defense mechanism is probably critical in

immunocompromised people, such people infected with human immunodeficiency virus, transplant recipients and patients with tumors.

METHODS

Mice. Dectin-1-knockout mice were generated by homologous recombination using the of embryonic stem cell line E14.1 (**Supplementary Methods** online). Dectin-1-knockout mice backcrossed for eight generations to BALB/cA mice (CLEA Japan) were used for *P. carinii* infection. For other experiments, unless stated otherwise in the figure legends, mice were backcrossed for eight generations to C57BL/6J mice (Nihon SLC). *Myd88*$^{-/-}$ mice were also backcrossed for more than eight generations to C57BL/6J mice[33]. Male or female mice 5–10 weeks of age were used for experiments, and wild-type C57BL/6J mice or BALB/cA mice were used as controls. All mice were kept in specific pathogen–free conditions at the Center for Experimental Medicine, The Institute of Medical Science, The University of Tokyo. Experiments were done according to institutional guidelines and were approved by institutional committees.

Cell preparation and β-glucan sensitivity analysis. Bone marrow cells were removed from the femurs and tibiae of 6- to 8-week-old female mice and BMDCs were prepared as described[34]. SCG (100 μg/ml) or LPS (20 ng/ml) was added on day 5 after cultivation with granulocyte-macrophage colony-stimulating factor and IL-4. On day 6, culture supernatants were collected for cytokine titration and nonadherent cells were used in cell surface marker expression assays. For isolation of alveolar macrophages, mouse lungs were lavaged with prewarmed PBS supplemented with 0.5 mM EDTA using an intratracheal catheter. Cells were collected and seeded (1.0×10^5 cells/ml), and nonadherent cells were removed 2 h later by washing in culture medium. Thereafter, NaClO-oxidized candida was added to the adherent cells, followed by culture for 24 h, and supernatants were then used for cytokine titration. For isolation of thioglycollate-elicited macrophages, mice were injected intraperitoneally with 2 ml of 4% (weight/volume) thioglycollate (Nissui). Then, 3 d later, peritoneal cells were collected by washing with PBS containing 0.5 mM EDTA. Total cells were then cultured for 2 d on a dish in RPMI 1640 medium supplemented with 10% (volume/volume) FCS; adherent cells were then used as thioglycollate-elicited macrophages.

Cytokine titration. Concentrations of IFN-γ, TNF, IL-10, and IL-12 were determined with a commercially available OptiEIA kit (BD Biosciences) according to the manufacturer's instructions.

Cell surface marker analysis. For analysis of cell surface markers on BMDCs, cells were cultured with or without stimulation as described above and then were analyzed by flow cytometry[35]. Antibodies used for detection were as follows: biotin-conjugated anti–mouse CD80 (16-10A1), biotin-conjugated anti–mouse CD40 (3/23), fluorescein isothiocyanate (FITC)–conjugated anti–mouse CD11c (HL3) and phycoerythrin-conjugated streptavidin were purchased from BD Bioscience, and biotin-conjugated monoclonal anti–mouse dectin-1 (RH1) was produced by immunization of rats with the recombinant carbohydrate-recognition domain of dectin-1. Fluorescence intensity was quantified with a FACSCalibur (BD) and data were analyzed with FlowJo software (Tree Star).

Preparation of β-glucans. SCG (β-1,6-branched β-1,3-glucan) was prepared from the fruit bodies of the edible mushroom *S. crispa* (Minahealth) as described[34]. NaClO-oxidized candida and insoluble β-1,6-branched β-1,3-glucans were prepared from *C. albicans* IFO1385 as described[36]. For conjugation with biotin, NaClO-oxidized candida (100 mg) was suspended in 5 ml of 0.1 M acetate buffer, pH 5.4. The suspension was mixed with 1.2 μmol sodium metaperiodate to partially oxidize branched 1, 6-linked glucosyl residues. The mixed suspension was further incubated for 1 h at 24 °C in the dark. NaClO-oxidized candida was washed with acetate buffer by centrifugation and then was mixed with 100 μg/ml of biotin (long arm) hydrazide (Vector Laboratories) dissolved in dimethysulfoxide and acetate buffer, followed by incubation for 1 h at 24 °C. The mixed NaClO-oxidized candida suspension was treated for 30 min with sodium borohydride. Biotin-conjugated NaClO-oxidized candida was washed with deionized water and then dried, with subsequent washing with ethanol, acetone and then diethyl ether. Biotin-labeled NaClO-oxidized candida was conjugated to FITC by incubation with streptavidin-FITC (BD Biosciences) before use. NaClO-oxidized zymosan was prepared as described[24]. Zymosan (1 g) was suspended for 1 d at 4 °C in 100 ml of 0.1 M NaOH with 0.5% NaClO. The insoluble fraction (NaClO-oxidized zymosan) was then collected by centrifugation and was suspended in 1 ml of saline and was sonicated for 30 s.

Assay for production of ROS. Production of ROS was analyzed by luminol-enhanced chemiluminescence. Thioglycollate-elicited macrophages (5×10^5 cells) isolated as described above were suspended in 1 ml culture medium and were incubated for 30 min at 37 °C. Aliquots (100 μl) were then placed in luminometer tubes and NaClO-oxidized zymosan (100 μg/ml) or zymosan (100 μg/ml) in 100 μl medium containing 100 μM luminol (Sigma) was added. Chemiluminescence was measured at 5-minute intervals with a luminometer (Lumat LB9507; Berthold Technologies). Chemiluminescence is expressed as relative luciferase units per minute per 1×10^3 cells.

***In vitro* binding assay.** Thioglycollate-elicited macrophages were collected from dectin-1-knockout mice, *Myd88*$^{-/-}$ mice and wild-type C57BL/6J mice (Nihon SLC) as described above. Cells were adjusted to a concentration of 5×10^5 cells/ml and 100 μl of the cell suspension was seeded onto a chamber slide system (Nalg Nunc International). Then, 2 h later, chambers were washed with culture medium and 100 μl of FITC-labeled NaClO-oxidized candida suspended in culture medium (100 μg/ml) or 100 μl of FITC-labeled *C. albicans* (1×10^5 cells) was added, followed by culture for 60 min. Unbound, unphagocytosed cells were then washed, followed by staining with CM-DiI (octadecyl indocarbocyanine (DiI) with a thiol-reactive chloromethyl moiety; Molecular Probes) and visualization with a confocal laser-scanning microscopy system (Radiance 2100; Nihon BIO RAD). For flow cytometry, thioglycollate-elicited macrophages and FITC-labeled NaClO-oxidized candida or FITC-labeled *C. albicans* were incubated for 60 min at 37 °C in polypropylene tubes. Then, cells were washed three times and were stained with CM-DiI or phycoerythrin-conjugated anti–mouse CD11b (M1/70; BD Biosciences). Fluorescence intensity was quantified with a FACSCalibur (BD Biosciences) and data were analyzed with FlowJo software (Tree Star).

T cell proliferation assay. $CD4^+$ T cells were isolated from lymph nodes and spleens of DO11.10 mice[37] or BALB/cA mice with an autoMACS (Miltenyi Biotec) after being stained with microbead-conjugated anti–mouse CD4 (Miltenyi Biotec) according to the manufacturer's instructions. DCs were also isolated with an autoMACS after being stained with microbead-conjugated anti–mouse CD11c (Miltenyi Biotec) from collagenase-digested spleens of dectin-1-knockout or dectin-1-wild-type mice on a BALB/cA background (fourth generation). $CD4^+$ T cells (1×10^5 cells) were cultured for 3 d in 96-well plates with DCs (1×10^4 cells) in the presence of ovalbumin peptide (amino acids 323–339) or anti–mouse CD3 purified from the culture supernatants of 145-2C11 cells (CRL-1975; American Type Culture Collection). Cells were incubated with [^{3}H]thymidine (0.25 mCi/ml; Amersham) for 6 h before collection, then incorporated radioactivity was measured with a Microbeta counter (Pharmacia Biotech)[38].

Immunization of mice and measurement of antibody titers. Mice (fourth generation on a BALB/cA background) were immunized intraperitoneally with 1×10^8 sheep red blood cells (Nihon Seibutsuzairyou) in PBS[39]. Blood samples were collected from tail veins both before immunization and 1 week after. Antigen-specific antibody titers were measured by enzyme-linked immunosorbent assay (ELISA) with plate-coated soluble sheep red blood cell antigens (2 mg/ml).

Delayed-type hypersensitivity response. Delayed-type hypersensitivity induced by methylated bovine serum albumin was assessed as described[40]. Footpad swelling was measured with a dial caliper and results were calculated as follows: footpad swelling (%) = (thickness of footpad injected with methylated bovine serum albumin) / (thickness of footpad injected with PBS) × 100.

***P. carinii* infection.** *P. carinii* was prepared from lung homogenates of BALB/c nude mice inoculated previously with *P. carinii*[41,42]. BALB/cA mice (dectin-1-wild-type or dectin-1-knockout) were inoculated intranasally with 1.7×10^4 cysts and mice were then killed at 7 d, 14 d, 20 d or 4 months after infection; cysts in the lungs were then counted. For experiments in immunocompromised conditions, anesthetized mice were inoculated with 6.4×10^5

cysts, followed by subcutaneous administration of cortisone acetate (Wako Pure Chemical Industries) at a dose of 2.5 mg per mouse twice weekly. *P. carinii* cysts in the lungs were counted as described[42], and total cysts on the smear were counted with a microscope after staining with toluidine blue O. The number of cysts per mouse was recorded. For *in vitro* cytokine production studies, alveolar macrophages at a density of 1×10^5 cells/ml were cultured for 2 h at 37 °C in 0.1 ml RPMI 1640 medium supplemented with 10% (volume/volume) FCS. After removal of nonadherent cells, adherent cells were incubated with 1×10^4 *P. carinii* cysts. Culture supernatants were then collected and cytokine concentrations were measured. Production of ROS was measured by luminol-enhanced chemiluminescence. Alveolar macrophages (4×10^5 cells) were isolated from dectin-1-knockout, *Myd88*$^{-/-}$ or wild-type C57BL/6J mice and were suspended in 1 ml of culture medium and incubated for 30 min at 37 °C. Aliquots (100 μl) were then placed in luminometer tubes and *P. carinii* (4×10^4 cysts) in 100 μl medium containing 100 μM luminol (Sigma) was added. Chemiluminescence was measured as described above.

***C. albicans* infection.** *C. albicans* (18804; American Type Culture Collection) was grown for 36 h at 30 °C on potato dextrose agar plates (Eiken Kizai). For survival analysis, wild-type and dectin-1-knockout mice were infected intravenously with 1×10^6 or 5×10^5 *C. albicans* and then were monitored for 20 d. Production of ROS was determined by the luminal-enhanced test as described above using alveolar macrophages (5×10^4 cells) and *C. albicans* (5×10^4 cells). For FITC labeling, 5 ml of a suspension of *C. albicans* (1×10^6 cells/ml) were incubated for 30 min at 24 °C with 0.1 mg/ml of FITC (Sigma) in PBS, and then cells were washed five times with PBS.

Statistics. Statistical significance was determined with a Mann-Whitney U-test and Student's *t*-test for analysis of *P. carinii* infection. Student's *t*-test was used for analysis of ELISAs and ROS assays, and a χ^2 test was used for analysis of survival assays.

Note: Supplementary information is available on the Nature Immunology website.

ACKNOWLEDGMENTS

DO11.10 mice were provided by D.Y. Loh (Washington University School of Medicine). Supported by Grants-in-Aid from the Ministry of Education, Culture, Sports, Science, and Technology of Japan and the Ministry of Health and Welfare of Japan (Y.I. and S.S.) and by the Japan Society for the Promotion of Science (N.F.).

AUTHOR CONTRIBUTIONS

S.S. mainly contributed throughout this work in collaboration with N.F., S.C. and K. Seki; H.K. and K. Sudo did embryonic stem cell culture and produced chimeric mice; Y.A. and N.O. made β-glucan preparations and did cytokine production experiments; T.F. did *in vivo P. carinii* experiments and provided *P. carinii* for the *in vitro* experiments; T.K., K.N. and K.K. did *in vivo C. albicans* experiments; S.A. provided *Myd88*$^{-/-}$ mice; and Y.I. supervised the study, designed the experiments and edited the draft paper.

COMPETING INTERESTS STATEMENT

The authors declare that they have no competing financial interests.

Published online at http://www.nature.com/natureimmunology/
Reprints and permissions information is available online at http://npg.nature.com/reprintsandpermissions/

1. Figdor, C.G., van Kooyk, Y. & Adema, G.J. C-type lectin receptors on dendritic cells and Langerhans cells. *Nat. Rev. Immunol.* **2**, 77–84 (2002).
2. Ariizumi, K. *et al.* Identification of a novel, dendritic cell-associated molecule, dectin-1, by subtractive cDNA cloning. *J. Biol. Chem.* **275**, 20157–20167 (2000).
3. Adachi, Y. *et al.* Characterization of β-glucan recognition site on C-type lectin, dectin 1. *Infect. Immun.* **72**, 4159–4171 (2004).
4. Taylor, P.R. *et al.* The β-glucan receptor, dectin-1, is predominantly expressed on the surface of cells of the monocyte/macrophage and neutrophil lineages. *J. Immunol.* **169**, 3876–3882 (2002).
5. Brown, G.D. & Gordon, S. Fungal β-glucans and mammalian immunity. *Immunity* **19**, 311–315 (2003).
6. Fitzpatrick, F.W., Haynes, L.J., Silver, N.J. & Dicarlo, F.J. Effect of glucan derivatives upon phagocytosis by mice. *J. Reticuloendothel. Soc.* **15**, 423–428 (1964).
7. Ross, G.D., Vetvicka, V., Yan, J., Xia, Y. & Vetvickova, J. Therapeutic intervention with complement and β-glucan in cancer. *Immunopharmacology* **42**, 61–74 (1999).
8. Steele, C. *et al.* Alveolar macrophage-mediated killing of *Pneumocystis carinii* f. sp. muris involves molecular recognition by the dectin-1 β-glucan receptor. *J. Exp. Med.* **198**, 1677–1688 (2003).
9. Gantner, B.N., Simmons, R.M. & Underhill, D.M. Dectin-1 mediates macrophage recognition of *Candida albicans* yeast but not filaments. *EMBO J.* **24**, 1277–1286 (2005).
10. Romani, L. Immunity to fungal infections. *Nat. Rev. Immunol.* **4**, 1–23 (2004).
11. Odds, F.C. *Candia and Candidosis* 2nd edn. (ed. Odds, F.C.) 252–278 (Baillere-Tindall, London, 1988).
12. Villamon, E., Roig, P., Gil, M.L. & Gozalbo, D. Toll-like receptor 2 mediates prostaglandin E_2 production in murine peritoneal macrophages and splenocytes in response to *Candida albicans*. *Res. Microbiol.* **156**, 115–118 (2005).
13. Tada, H. *et al. Saccharomyces cerevisiae*- and *Candida albicans*-derived mannan induced production of tumor necrosis factor α by human monocytes in a CD14- and Toll-like receptor 4-dependent manner. *Microbiol. Immunol.* **46**, 503–512 (2002).
14. Stahl, P.D. & Ezekowitz, R.A. The mannose receptor is a pattern recognition receptor involved in host defense. *Curr. Opin. Immunol.* **10**, 50–55 (1998).
15. Lee, S.J., Zheng, N.Y., Clavijo, M. & Nussenzweig, M.C. Normal host defense during systemic candidiasis in mannose receptor-deficient mice. *Infect. Immun.* **71**, 437–445 (2003).
16. Swain, S.D., Lee, S.J., Nussenzweig, M.C. & Harmsen, A.G. Absence of the macrophage mannose receptor in mice does not increase susceptibility to *Pneumocystis carinii* infection *in vivo*. *Infect. Immun.* **71**, 6213–6221 (2003).
17. Ohno, N., Miura, N.N., Nakajima, M. & Yadomae, T. Antitumor 1,3-β-glucan from cultured fruit body of *Sparassis crispa*. *Biol. Pharm. Bull.* **23**, 866–872 (2000).
18. Di Carlo, F.J. & Fiore, J.V. On the composition of zymosan. *Science* **127**, 756–757 (1958).
19. Kopp, E.B. & Medzhitov, R. The Toll-receptor family and control of innate immunity. *Curr. Opin. Immunol.* **11**, 13–18 (1999).
20. Gantner, B.N., Simmons, R.M., Canavera, S.J., Akira, S. & Underhill, D.M. Collaborative induction of inflammatory responses by dectin-1 and Toll-like receptor 2. *J. Exp. Med.* **197**, 1107–1117 (2003).
21. Brown, G.D. *et al.* Dectin-1 mediates the biological effects of β-glucans. *J. Exp. Med.* **197**, 1119–1124 (2003).
22. Underhill, D.M. *et al.* The Toll-like receptor 2 is recruited to macrophage phagosomes and discriminates between pathogens. *Nature* **401**, 811–815 (1999).
23. Kawai, T., Adachi, O., Ogawa, T., Takeda, K. & Akira, S. Unresponsiveness of MyD88-deficient mice to endotoxin. *Immunity* **11**, 115–122 (1999).
24. Hida, S., Nagi-Miura, N., Adachi, Y. & Ohno, N. Beta-glucan derived from zymosan acts as an adjuvant for collagen-induced arthritis. *Microbiol. Immunol.* **50**, 453–461 (2006).
25. Pollock, J.D. *et al.* Mouse model of X-linked chronic granulomatous disease, an inherited defect in phagocyte superoxide production. *Nat. Genet.* **9**, 202–209 (1995).
26. Edwards, A.D. *et al.* Microbial recognition via Toll-like receptor-dependent and -independent pathways determines the cytokine response of murine dendritic cell subsets to CD40 triggering. *J. Immunol.* **169**, 3652–3660 (2002).
27. Smits, G.J., Kapteyn, J.C., van den Ende, H. & Klis, F.M. Cell wall dynamics in yeast. *Curr. Opin. Microbiol.* **2**, 348–352 (1999).
28. Hanano, R., Reifenberg, K. & Kaufmann, S.H. Activated pulmonary macrophages are insufficient for resistance against *Pneumocystis carinii*. *Infect. Immun.* **66**, 305–314 (1998).
29. Rudmann, D.G., Preston, A.M., Moore, M.W. & Beck, J.M. Susceptibility to *Pneumocystis carinii* in mice is dependent on simultaneous deletion of IFN-γ and type 1 and 2 TNF receptor genes. *J. Immunol.* **161**, 360–366 (1998).
30. Rogers, N.C. *et al.* Syk-dependent cytokine induction by dectin-1 reveals a novel pattern recognition pathway for C type lectins. *Immunity* **22**, 507–517 (2005).
31. Mansour, M.K. & Levitz, S.M. Interactions of fungi with phagocytes. *Curr. Opin. Microbiol.* **5**, 359–365 (2002).
32. Netea, M.G. *et al.* Immune sensing of *Candia albicans* require cooperative recognition of mannans and glucans by lectin and Toll-like receptors. *J. Clin. Invest.* **116**, 1642–1650 (2006).
33. Adachi, O. *et al.* Targeted disruption of the MyD88 gene results in loss of IL-1- and IL-18-mediated function. *Immunity* **9**, 143–150 (1998).
34. Harada, T. *et al.* IFN-gamma induction by SCG, 1,3-β-D-glucan from *Sparassis crispa*, in DBA/2 mice *in vitro*. *J. Interferon Cytokine Res.* **22**, 1227–1239 (2002).
35. Saijo, S., Asano, M., Horai, R., Yamamoto, H. & Iwakura, Y. Suppression of autoimmune arthritis in interleukin-1-deficient mice in which T cell activation is impaired due to low levels of CD40 ligand and OX40 expression on T cells. *Arthritis Rheum.* **46**, 533–544 (2002).
36. Ishibashi, K. *et al.* Relationship between the physical properties of *Candida albicans* cell well β-glucan and activation of leukocytes *in vitro*. *Int. Immunopharmacol.* **2**, 1109–1122 (2002).
37. Shinkai, Y. *et al.* Restoration of T cell development in RAG-2-deficient mice by functional TCR transgenes. *Science* **259**, 822–825 (1993).
38. Habu, K. *et al.* The human T cell leukemia virus type I-tax gene is responsible for the development of both inflammatory polyarthropathy resembling rheumatoid arthritis and noninflammatory ankylotic arthropathy in transgenic mice. *J. Immunol.* **162**, 2956–2963 (1999).
39. Nakae, S., Asano, M., Horai, R. & Iwakura, Y. Interleukin-1β, but not interleukin-1α, is required for T-cell-dependent antibody production. *Immunology* **104**, 402–409 (2001).
40. Nakae, S. *et al.* Antigen-specific T cell sensitization is impaired in IL-17-deficient mice, causing suppression of allergic cellular and humoral responses. *Immunity* **17**, 375–387 (2002).
41. Furuta, T., Ueda, K., Kyuwa, S. & Fujiwara, K. Effect of T-cell transfer on *Pneumocystis carinii* infection in nude mice. *Jpn. J. Exp. Med.* **54**, 57–64 (1984).
42. Furuta, T. *et al.* Therapeutic effects of water-soluble echinocandin compounds on *Pneumocystis pneumonia* in mice. *Antimicrob. Agents Chemother.* **42**, 37–39 (1998).

JOURNAL OF VIROLOGY, Jan. 2007, p. 677–688 Vol. 81, No. 2
0022-538X/07/$08.00+0 doi:10.1128/JVI.00870-06

Nuclear Import of the Preintegration Complex Is Blocked upon Infection by Human Immunodeficiency Virus Type 1 in Mouse Cells[▽]

Naomi Tsurutani,[1]† Jiro Yasuda,[1,2] Naoki Yamamoto,[3] Byung-Il Choi,[1] Motohiko Kadoki,[1] and Yoichiro Iwakura[1]*

Center for Experimental Medicine, Institute of Medical Science, University of Tokyo, Tokyo 108-8639,[1] Fifth Biology Section for Microbiology, Department of First Forensic Science, National Research Institute of Police Science, Kashiwa 277-0882,[2] and Department of Molecular Virology, School of Medicine, Tokyo Medical and Dental University, Tokyo 113-8510,[3] Japan

Received 28 April 2006/Accepted 17 October 2006

Mouse cells do not support human immunodeficiency virus type 1 (HIV-1) replication because of host range barriers at steps including virus entry, transcription, RNA splicing, polyprotein processing, assembly, and release. The exact mechanisms for the suppression, however, are not completely understood. To elucidate further the barriers against HIV-1 replication in mouse cells, we analyzed the replication of the virus in lymphocytes from human CD4/CXCR4 transgenic mice. Although primary splenocytes and thymocytes allowed the entry and reverse transcription of HIV-1, the integration efficiency of the viral DNA was greatly reduced in these cells relative to human peripheral blood mononuclear cells, suggesting an additional block(s) before or at the point of host chromosome integration of the viral DNA. Preintegration processes were further analyzed using HIV-1 pseudotyped viruses. The reverse transcription step of HIV-1 pseudotyped with the envelope of murine leukemia virus or vesicular stomatitis virus glycoprotein was efficiently supported in both human and mouse cells, but nuclear import of the preintegration complex (PIC) of HIV-1 was blocked in mouse cells. We found that green fluorescent protein (GFP)-labeled HIV-1 integrase, which is known to be important in the nuclear localization of the PIC, could not be imported into the nucleus of mouse cells, in contrast to human cells. On the other hand, GFP-Vpr localized exclusively to the nuclei of both mouse and human cells. These observations suggest that, due to the dysfunction of integrase, the nuclear localization of PIC is suppressed in mouse cells.

A small animal model for AIDS would provide a valuable tool for the study of its pathogenesis and the evaluation of vaccine candidates and antiviral drugs. However, attempts to produce small animal models have been hampered thus far by species-specific host range barriers to infection by human immunodeficiency virus type 1 (HIV-1). CD4, the cellular receptor for HIV-1 (41, 49), was first identified as a host range barrier because mouse CD4 (muCD4) does not bind HIV-1 Env (46). Human CD4 (huCD4) transgenic (Tg) mice, however, were not susceptible to HIV-1 infection, suggesting the presence of additional barriers (47). Chemokine receptors were later identified as entry coreceptors (9, 22), but primary lymphocytes from mice transgenic for huCD4 and either huCXCR4 (70) or huCCR5 (13) exhibited little to no signs of productive infection.

Cyclin T1 (CycT1) is responsible for a transcriptional level barrier (3, 4, 26, 30, 58). CycT1 protein is a component of the TAK/pTEFb transcription factor complex (51, 78), and huCycT1 binds Tat and activates transcription from the promoter in the long terminal repeat (LTR). However, muCycT1 cannot bind Tat. Nevertheless, introduction of the huCycT1 protein to rodent cells together with a mixture of human receptors was insufficient to induce productive viral infection (11, 52).

Additional barriers have been reported in the late steps of the viral life cycle (11, 27, 40, 42, 43, 53). These late-stage defects can be rescued by fusing HIV-1-infected rodent cells to uninfected human cells (11, 52), indicating that the defects are due to the lack of necessary factors in rodent cells rather than the presence of dominant inhibitors of HIV-1 replication. CRM1, a nuclear export factor that functions in association with Rev, and p32, a splicing inhibitor and Rev-binding protein, are suggested to be necessary late-phase factors (67, 83).

We previously produced Tg mice carrying the HIV-1 proviral genome in which the *pol* gene is deleted (HIV-Tg) (36). Although transgene expression in lymphoid tissues is barely detectable under normal physiological conditions, relatively high levels of p24 Gag protein were detected in the serum (up to 400 pg/ml) after injection of bacterial lipopolysaccharide (74). All mRNA species, including unspliced, singly spliced, and multiply spliced mRNAs were produced normally. Thus, once the viral genome is integrated into the host chromosome, viral genes are expressed at a reasonable efficiency even in mouse cells, suggesting that the major host range barriers are present in the early stage of infection (prior to viral DNA integration) rather than in the late stage. However, it is not yet known whether there are any additional host range barriers in the early steps.

* Corresponding author. Mailing address: Center for Experimental Medicine, Institute of Medical Science, University of Tokyo, 4-6-1 Shirokanedai, Minato-ku, Tokyo 108-8639, Japan. Phone: 81 3 5449 5536. Fax: 81 3 5449 5430. E-mail: iwakura@ims.u-tokyo.ac.jp.

† Present address: Laboratory of Viral Infection II, Kitasato Institute for Life Sciences, Kitasato University, Tokyo 108-8641, Japan.

▽ Published ahead of print on 1 November 2006.

In this report, we investigated additional barrier steps of HIV-1 replication in mouse cells and found that the efficiency of viral genome integration into the host chromosome was low in huCD4/CXCR4 Tg mice. As this result suggested an additional barrier in the early steps of viral infection, we examined nuclear transport of the viral genome and demonstrated that integrase (IN)-dependent nuclear import of the preintegration complex (PIC) is blocked in mouse cells.

MATERIALS AND METHODS

Transgene construction. The huCD4 Tg vector (pCT4) was constructed as follows. The 0.85-kb XhoI-EcoRV fragment containing the muCD4 enhancer/promoter was ligated to a 1.8-kb EcoRV-HindIII fragment containing the huCD4 open reading frame, and then a 1.95-kb HindIII-SpeI fragment containing a rabbit β-globin intron sequence and a simian virus 40 (SV40) polyadenylation [poly(A)] signal was inserted into the HindIII-SpeI site downstream of the huCD4 gene (29) (Fig. 1A). To construct the huCXCR4 Tg vector, an XhoI-NotI fragment containing the entire coding region of huCXCR4 was isolated from pBCMGSNeo/HM89 (61), and the huCXCR4 fragment was blunted by T4 DNA polymerase, followed by insertion into the EcoRV site of pCDGH. pCDGH consisted of the muCD4 enhancer/promoter and a human growth hormone gene with its poly(A) signal but devoid of its initiation codon (pCFG) (80) (Fig. 1A). The XhoI-SpeI fragment from pCT4 and the XhoI-NotI fragment from pCFG were then purified and coinjected into the male pronuclei of fertilized mouse eggs (C3H/HeN) (80). The transgenes were detected by dot blot hybridization using DNA prepared from mouse tails (34). Mice were kept under specific-pathogen-free conditions in an environmentally controlled clean room at the Center for Experimental Medicine, the Institute of Medical Science, the University of Tokyo. All equipment and supplies were sterilized, including the cages, water bottles, wood chips, and food pellets. All experiments were conducted according to the institutional ethical and safety guidelines for animal experiments and safety guidelines for gene manipulation experiments.

Northern blot hybridization. Northern blot analyses were carried out as previously described (80). The EcoRV-SpeI fragment of huCD4 and the XhoI-NotI fragment of huCXCR4 used for transgene construction were used as templates to make probes detecting huCD4 and huCXCR4 mRNA, respectively. The autoradiograms were developed, and the radioactivity of each band was quantified with a BAS 2000 Bio-Image analyzer (Fuji Film, Tokyo, Japan).

Plasmids. The HIV-1 pNL4-3 (X4-tropic, accession no. M19921) vector was obtained from A. Adachi (1). The HIV-1 pNL43lucΔenv vector, in which the *env* gene is defective and the *nef* gene is replaced by the firefly luciferase (*Luc*) gene, the pNL4-3 vector containing a mutation at the IN catalytic site (D116G), and an amphotropic Moloney murine leukemia virus (MuLV) envelope expression vector (pJD-1) were kindly provided by T. Masuda (54, 65, 76). A vesicular stomatitis virus G (VSV-G)-expressing plasmid (pMD-G) was obtained from L. Naldini (5, 62). The pGEM/NL-2-LTR plasmid was kindly provided by Y. Koyanagi (73).

The HIV-1 pNL43lucΔenv vector carrying a IN protein tagged with the SV40 nuclear localization signal (NLS) was constructed by using overlap extension PCR (33). First, two different PCRs were performed using HIV-1 pNL43lucΔenv vector as the template: one with the AflII-sense primer, 5′-CATCTTAAGACA GCAGTACAAATGGCAGTA-3′, and NLS-antisense primer, 5′-GGCCTTTC TCTTCTTTTTTGGATCCTCATCCTGTCTACTTGCC-3′, and the other with the NLS-sense primer, 5′-CCAAAAAAGAAGAGAAAGGCCTAACACATG GAAAAGATTAGT-3′, and PflMI-antisense primer, 5′-CTCTTTTTCCTCCA TTCTATGGAGACTCCCTG-3′. These two PCR amplicons were then combined and used as the template for the third PCR with outer primers AflII-sense and PflMI-antisense. The final PCR product was digested with AflII and PflMI and ligated to the SpeI/AflII and SpeI/PflMI vector fragments of HIV-1 pNL43lucΔenv. The nucleotide sequence of the construct was confirmed by sequencing.

To prepare the expression vector for HIV-1 IN N-terminal fusion to enhanced green fluorescence protein (EGFP) (GFP-IN), the entire coding region of HIV-1 IN was amplified by PCR and inserted into the pEGFP-C2 expression vector (Clontech Laboratories, Palo Alto, CA) at its EcoRI and ApaI sites. The primers used to amplify the HIV IN were GFP-IN-sense, 5′-CCGGAATTCCGGGCC ATAGCGGCCTTTTTAGATGGAATAGAT-3′, and GFP-IN-antisense, 5′-TC CGGGCCCGGATTAATCCTCATCCTGTCTACT-3′. To generate the expression vector for the HIV-1 Vpr N or C terminus fused to EGFP (GFP-Vpr, Vpr-GFP), the entire coding region of HIV-1 Vpr was amplified by PCR and inserted into the pEGFP-C2 or pEGFP-N1 expression vector at the HindIII and ApaI or HindIII and BamHI sites, respectively. The primers used to amplify HIV-1 Vpr were GFP-Vpr-sense, 5′-CCCAAGCTTGGGGGACGCCATGGA ACAAGCCCCAGAA-3′, and GFP-Vpr-antisense, 5′-TCCGGGCCCGGACT AGGATCTACTGGCTCCATT-3′, or Vpr-GFP-sense, 5′-CCCAAGCTTGGG GACATGGAACAAGCCCCAGAA-3′, and Vpr-GFP-antisense, 5′-CGCGGA TCCGCGGAGGATCTACTGGCTCCATT-3′, respectively. The amplified regions and the cloning junctions were confirmed by DNA sequencing.

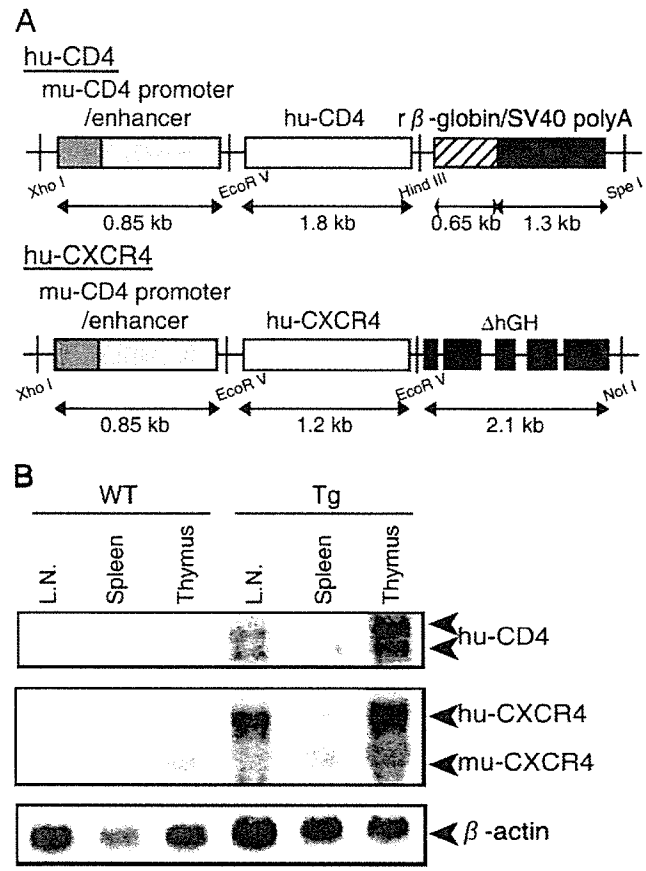

FIG. 1. (A) Transgene constructs. huCD4 or CXCR4 cDNA was placed downstream of the muCD4 enhancer/promoter and ligated to the SV40 poly(A) signal (huCD4) or to a defective human growth hormone gene containing the poly(A) signal (huCXCR4). (B) Transgene expression in lymphatic organs. Northern blot hybridization analysis was performed using 10 μg of total RNA prepared from the thymus, spleen, or lymph nodes of WT or Tg mice. The positions expected for huCD4, huCXCR4, muCXCR4, and β-actin mRNA are indicated on the right.

Cell culture and isolation of human PBMCs and mouse splenocytes and thymocytes. Human fibroblast-like cell lines (293T and HeLa), a mouse embryo fibroblast-like cell line (NIH 3T3) derived from an NIH Swiss mouse (Fv-1^n), and a mouse rectum carcinoma cell line (Colon-26) from a BALB/c mouse (Fv-1^b) were cultured in Dulbecco's modified Eagle's medium (Invitrogen, Tokyo, Japan) supplemented with 10% fetal bovine serum (FBS). The Colon-26 cell line was obtained provided from the Cell Resource Center for Biomedical Research Institute of Development, Aging, and Cancer, Tohoku University, Japan (75). Human T-cell lymphoma cell lines (MT-4 and Jurkat) and mouse T-cell lymphoma cell lines (EL4, YAC-1, and BW5147) were cultured in RPMI 1640 (SIGMA, Tokyo, Japan) containing 10% FBS. Human peripheral blood mononuclear cells (PBMCs) were obtained from peripheral blood. Briefly, buffy coats from the peripheral blood of healthy HIV-seronegative blood donors were separated over a Ficoll-Hypaque gradient (Ficoll-Paque PLUS; GE Healthcare Bio-Sciences, Tokyo, Japan). C3H/HeN mice (Charles River, Tokyo, Japan) were sacrificed at 8 weeks, and the splenocytes and thymocytes were isolated by passage through nylon mesh. Human PBMC suspensions and mouse splenocytes

and thymocytes were stimulated with 1% phytohemagglutinin (SIGMA, Tokyo, Japan). These cells were grown in RPMI 1640 medium containing 4 ng/ml of recombinant human interleukin 2 or mouse interleukin 2 (Peprotech EC Ltd, London, United Kingdom) per ml and 10% FBS. After 1 week, human PBMCs and mouse splenocytes and thymocytes were >96% T cells and >40% activated cells, as judged by fluorescence-activated cell sorter analysis using anti-CD3 or anti-CD69 monoclonal antibodies (BD Biosciences, Tokyo, Japan), respectively (data not shown).

Virus preparation and infection assays. HIV-1 strain NL4-3 was propagated in MT-4 cells, and the supernatants were filtered and stored at −80°C until use. For single-round infection assays, pseudotyped viruses were generated by cotransfection of 293T cells with pNL43lucΔenv vector and an amphotropic Moloney MuLV envelope expression vector (pJD-1) or a VSV-G envelope expression vector (pMD-G) using Lipofectamine PLUS (Invitrogen) (76). The pNL43lucΔenv vector containing a mutation at the IN catalytic site (D116G) was used as a control (54). The culture supernatants of the transfected 293T cells were harvested at 48 h posttransfection, filtered through 0.45-μm filters, and used as the virus preparations. Each virus preparation was treated with DNase I (40 μg/ml; Worthington Biochemical Co., Lakewood, NJ) in the presence of 10 mM $MgCl_2$ at 37°C for 1 h to avoid DNA contamination. An aliquot of each virus preparation was incubated at 65°C for 1 h and used as a heat-inactivated control. To monitor viral gene expression from the pNL43lucΔenv vector carrying a IN protein tagged with the SV40 NLS, luciferase activity in transfected 293T cells was measured on a Lumat LB9507 luminometer (BERTHOLD, Technologies, Bad Wildbad, Germany). At 48 h posttransfection, 293T cells were lysed with 1 ml of luciferase lysis buffer (Promega). One microliter of each cell lysate was subjected to the luciferase assay. Human PBMCs (5×10^6) or HeLa (5×10^5), MT-4 (5×10^6), Jurkat (5×10^6), mouse splenocytes (5×10^6), mouse thymocytes (5×10^6), NIH 3T3 (5×10^5), BW5147 (5×10^6), EL4 (5×10^6), or YAC-1 (5×10^6) cells were infected with an aliquot (2 ml; containing approximately 500 ng [NL4-3], 200 ng [HIV-1/MuLV], or 50 ng [HIV-1/VSV-G] of p24) of DNase-treated virus. The infection proceeded in the presence of Polybrene (SIGMA, Tokyo, Japan) (10 μg/ml) at 37°C. After 6 h, the viruses were removed, and the cells were overlaid with fresh media and incubated at 37°C. For p24 CA analysis, the infected cell supernatants were removed on the indicated days following infection. The levels of HIV-1 p24 antigen were determined by an enzyme immunoassay system (RETRO-TEK; ZeptoMetrix Corp., Buffalo, NY). For luciferase analysis, infected cells were harvested 4 days after infection, and the total cell pellets from each well were washed twice with phosphate-buffered saline (PBS) and lysed in luciferase lysis buffer (Promega). Luciferase activity (measured in a relative light units [RLU]) was measured on a Lumat LB9507 luminometer (BERTHOLD, Technologies, Bad Wildbad, Germany).

Analysis of HIV-1 DNA synthesis and formation of 2-LTR circles. Cells were harvested 24 h after infection. After washing with PBS, nucleic acids were extracted as described previously (81). Briefly, cells were disrupted in urea lysis buffer (4.7 M urea, 1.3%, sodium dodecyl sulfate [SDS], 0.23 M NaCl, 0.67 mM EDTA, and 6.7 mM Tris-HCl [pH 8.0]), phenol-chloroform extracted, and ethanol precipitated. The DNA pellet was resuspended in distilled H_2O, and an aliquot of each sample was analyzed by PCR. For ex vivo infection of primary lymphocytes from huCD4/CXCR4 Tg mice, partial reverse transcripts of the viral DNA were quantified by semiquantitative PCR. The primers used were as follows (37, 45, 81): R-U5, R, 5′-GCCTCAATAAAGCTTGCCTTG-3′ (sense, positions 522 to 542); U5, 5′-CCACTGCTAGAGATTTTCCAC-3′ (antisense, positions 616 to 638); Gag forward, 5′-TGGGGGGACATCAAGCAGCCATG CA-3′ (sense, positions 1360 to 1385); Gag reverse, 5′-CTATGTCACTTCCCC TTGGTTCTCT-3′ (antisense, positions 1474 to 1498). The PCR program was 30 cycles at 95°C for 1 min, 60°C for 1 min, and 72°C for 1 min in the presence of [^{32}P]dCTP. The PCR products were electrophoresed on an 8% polyacrylamide–Tris-borate-EDTA gel. The autoradiograms were developed, and the radioactivity of each band was quantified by a BAS 2000 Bio-Image analyzer. For single-round infections, the DNA was measured by quantitative PCR using an ABI PRISM 7900HT qPCR machine (Applied Biosystems, Tokyo, Japan). The PCR primer pairs were as follows: R-U5 (M667/AA55), R-gag (M667/M661) (76), and the 2-LTR junction's sequence (2-LTR-S/2-LTR-AS) (73). The cycling conditions included a hot start (50°C for 2 min, 95°C for 10 min), followed by 40 cycles of denaturation (95°C for 15 s) and extension (60°C for 1 min). To compensate for varying DNA sample recovery, the data are presented as ratios of HIV-1 DNA to β-actin DNA.

Cassette ligation-mediated PCR and integration analysis. For the detection of the HIV-1 integration form, we designed a cassette ligation-mediated PCR system using an in vitro LA cloning kit (TaKaRa BIO, Shiga, Japan) (35) (see Fig. 3A). Briefly, 5 μg of DNA was digested with EcoRI and ligated to double-stranded DNA cassettes with compatible ends. The cassette-ligated restriction fragments were then subjected to two rounds of PCR using the cassette- and HIV-specific primers C1 (5′-GTACATATTGTCGTTAGAACGCGTAATACG ACTCA-3′) and Gag reverse (described above) for the cassette, *gag*, and its upstream region and C2 (5′-CGTTAGAACGCGTAATACGACTCACTATAG GGAGA-3′) and U5 reverse (described above) for the cassette sequence downstream of C1 and the LTR region. PCR was performed according to the manufacturer's instructions. The amplification conditions were 30 cycles of 1 min at 94°C, 2 min at 54°C, 2 min at 72°C, and a final extension of 1 min at 72°C. The amplified products were resolved on 2% agarose gels and stained with SYBR green (FMC Bioproduct, Rockland, ME).

Fluorescence microscopy. HeLa (4×10^4), NIH 3T3 (3×10^4), and Colon-26 (3×10^4) cells were seeded onto 8-well culture slides (Nalge Nunc International, Rochester, NY) and transfected with the indicated plasmids using Lipofectamine 2000 (Invitrogen). At 24 h posttransfection, the cells were washed once in PBS and fixed with acetone for 5 min. After washing with PBS, the cells were mounted in 90% glycerol–50 mM $NaHCO_3$-Na_2CO_3 and covered by a coverslip. Confocal microscopy was performed with a Nikon Optiphot-2 fluorescence microscope with a Bio-Rad MRC 1024 laser confocal imaging system, and the digital images were prepared using Adobe Photoshop software.

Particle preparation and Western blot analysis. The culture supernatant (5 ml) of HIV-1 producing plasmid-transfected 293T cells was collected at 48 h postinfection. It was centrifuged thorough 20% (wt/vol) sucrose–PBS in an SW55 rotor (Beckman Coulter) at 4°C at 147,000 × *g* for 2 h (56), and the pellet was resuspended in PBS. The viral pellets were hearted at 90°C for 10 min in the presence of sample buffer (62.5 mM Tris-HCl, pH 6.8, 10% glycerol, 2% SDS, 5% 2-mercaptoethanol, 0.005% bromophenol blue). Then viral proteins were electrophoresed on a 12% SDS–polyacrylamide gel containing 0.2% SDS. Following blotting of proteins onto a polyvinylidene difluoride membrane, the membrane was first incubated with an antiserum from an AIDS patient (provided by Y. Inagaki, Tokyo Medical and Dental University, Tokyo, Japan, and Y. Koyanagi, Kyoto University, Kyoto, Japan), followed by horseradish peroxidase-conjugated anti-human immunoglobulin. HIV-1 proteins were visualized using an enhanced chemiluminescence detection system (GE Healthcare Bio-Science, Tokyo, Japan).

Statistical analysis. Data were analyzed using Excel and Student's *t* test. A *P* value of <0.05 was considered statistically significant, and all results are presented as means ± standard errors of the means (SEM).

RESULTS

Lymphocytes from huCD4/CXCR4 Tg mice do not fully support HIV-1 infection. To elucidate the host range barriers of HIV-1 replication in mice, we analyzed the early processes of HIV-1 infection in huCD4/CXCR4 Tg mouse splenocytes. Transgenic mice were generated by introducing both huCD4 and huCXCR4 cDNA along with the muCD4 enhancer/promoter into fertilized C3H mouse eggs (Fig. 1A). As shown in Fig. 1B, the huCD4 and huCXCR4 mRNAs were detected mostly in the thymus but also in the lymph nodes and spleen. Two huCD4 mRNA species were detected due to alternative splicing of the SV40 gene that was ligated to the huCD4 gene (Fig. 1B). fluorescence-activated cell sorter analyses showed that Tg splenocytes and thymocytes both expressed huCD4 and huCXCR4 on their cell surfaces (data not shown).

To examine the susceptibility of these Tg mice to HIV infection, splenocytes and thymocytes were isolated from the mice and infected with T-tropic HIV-1 (NL4-3) or M-tropic HIV-1 (JR-CSF). However, we could not detect any p24 antigen in the culture supernatant of these Tg mouse-derived cells, although significant levels of p24 (up to 80 pg/ml) were produced in human PBMC culture supernatant 12 days after infection.

To determine the process by which the viral replication is blocked, we analyzed the early infection steps by examining the viral genomic structure. Twenty-four hours after HIV-1 infection of the huCD4/CXCR4 Tg splenocytes, cells were har-

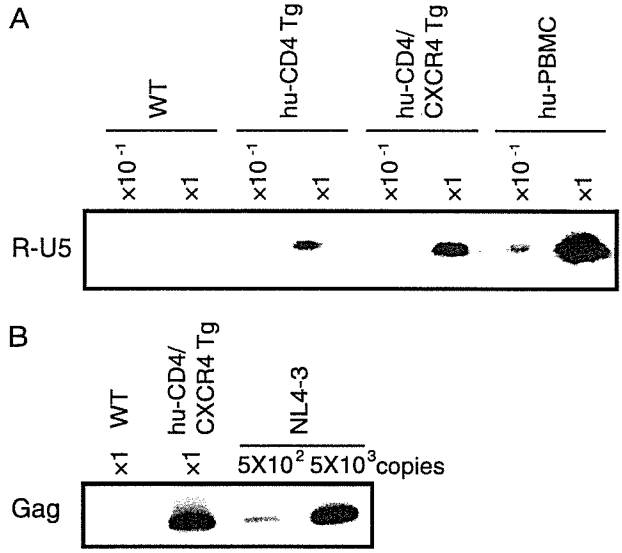

FIG. 2. HIV infection of splenocytes and thymocytes of WT and huCD4/CXCR4 Tg mice. Splenocytes or thymocytes from WT mice, Tg mice, or human PBMCs were isolated and infected with equivalent amounts of DNase-treated NL4-3 virus at 37°C for 6 h. After 6 h, the viruses were removed and the cells were treated with trypsin (500 μg/ml) at 37°C for 10 min and then washed in growth medium. (A and B) Splenocytes were harvested at 24 h postinfection. Total DNA was extracted from the cells and subjected to PCR analysis with a primer pair for R/U5 (A) or R/gag (B). The reaction was carried out using the DNA preparation from 1×10^5 cells (×1) or 1×10^4 cells ($\times 10^{-1}$). In panel B, the lanes marked 5×10^2 and 5×10^3 represent PCR products using 5×10^2 or 5×10^3 copies of the pNL4-3 plasmid as the template.

vested and total DNA was extracted. Early (R-U5) and late-infectious intermediate products (R-gag) were determined using semiquantitative PCR with specific primers. As shown in Fig. 2A and B, both infectious intermediates were detected specifically in the DNA isolated from the splenocytes of huCD4/CXCR4 Tg mice exposed to HIV-1, indicating that viral entry and reverse transcription had proceeded normally in mouse cells provided that human viral receptors were supplied. Similar results were also obtained in huCD4/CCR5 Tg mouse splenocytes infected with HIV-1 JR-CSF (data not shown). In contrast, the early infectious intermediate was not detected in wild-type mouse splenocytes, indicating a block upon viral entry. Taken together, these results suggest that HIV-1 replication in huCD4/CXCR4 Tg splenocytes was blocked later than the reverse transcription step(s).

HIV-1 infection of mouse cells is blocked at steps preceding integration into the host chromosome. We next examined the integration of the HIV-1 genome into the host chromosome. The pNL4-3 vector containing a mutation at the IN catalytic site (D116G) was used as a control (54). DNA from the infected cells was digested with EcoRI, which cut proviral DNA at only one site (nucleotide number 5743 of NL4-3, accession no. M19921). The DNA was then ligated to an EcoRI-specific cassette and subjected to the first round of PCR using primers specific for the cassette and the *gag* region, followed by the second round of PCR using primers for the cassette and the LTR region (Fig. 3A). As a result, the integrated viral DNA was visualized as smearing bands greater than 638 bp, which is

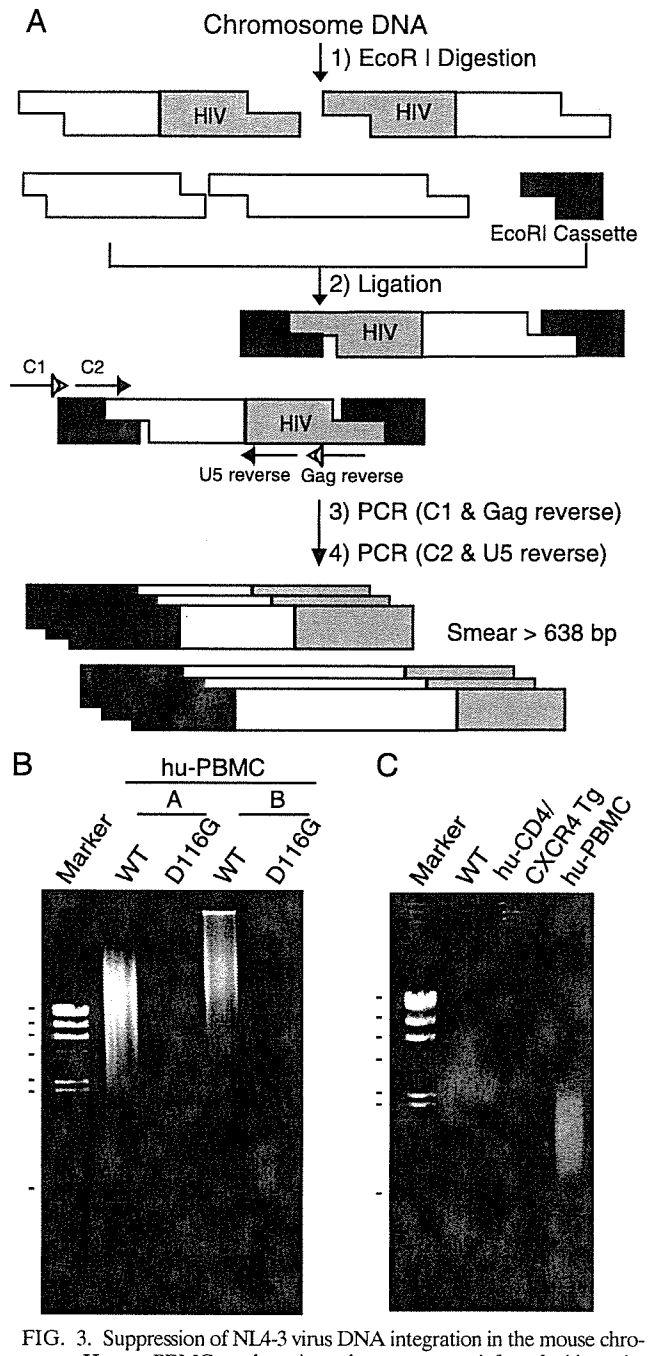

FIG. 3. Suppression of NL4-3 virus DNA integration in the mouse chromosome. Human PBMCs and murine splenocytes were infected with equivalent doses of DNase-treated NL4-3 virus. After 6 h, the virus was removed and the cells were washed with growth medium. At 1 day postinfection, the cells were harvested and used to extract total DNA. The DNA (5 μg) was digested with EcoRI and ligated to double-stranded DNA cassettes with compatible ends. The cassette-ligated DNA fragments were used as templates for nested PCR using cassette- and HIV-specific primers. (A) Schematic representation of cassette ligation-mediated PCR and the primers used to detect HIV integration into the host chromosome. (B and C) Detection of the chromosome-integrated forms of viral DNA. (B) Human PBMC preparations from two donors (A and B) were infected with NL4-3-WT or integrase mutant (D116G), and the DNAs were subjected to PCR analysis. Markers: 23.1, 9.4, 6.6, 4.3, 2.3, 2.0, and 0.564 kb (λ/HindIII). (C) DNA was isolated from NL4-3-infected splenocytes or thymocytes from WT or Tg mice or human PBMCs following infection and subjected to PCR analysis. Note the smearing bands in virus-infected human PBMCs but not in huCD4/CXCR4 Tg mice. Marker: λ/HindIII.

the original length between C2 and U5 reverse primers without insertion. Smearing bands were clearly detected when the DNA from HIV-1 wild type (WT)-infected human PBMCs was analyzed. In contrast, no smearing bands were detected with the DNA from HIV-1-D116G infected human PBMC, HIV-1-WT infected splenocytes from WT, and huCD4/CXCR4 transgenic mice (Fig. 3B and C). These results suggest that HIV-1 replication is also blocked in mouse cells at steps between the entry and viral DNA integration steps or at the viral integration step in addition to the adhesion/entry step.

The infection of mouse cells with both HIV-1/pJD-1 and HIV-1/VSV-G pseudotyped virus are blocked at a postentry step. To examine the possibility that HIV-1 replication in mouse cells is blocked at steps between the viral entry and DNA integration steps, we analyzed the early steps of viral infection using HIV-1 pseudotyped viruses in which the Env is replaced by an amphotropic MuLV Env (HIV-1/pJD-1) or by the G protein of VSV (HIV-1/VSV-G) and the *nef* gene is replaced by the firefly luciferase gene (76). The MuLV envelope pseudotype uses a ubiquitously expressed phosphate transporter as the receptor (55), and the VSV-G envelope pseudotype is capable of infecting cells through a carbohydrate receptor and the endocytic pathway (2). By using these pseudotyped viruses, we overcame the barriers at the adhesion and entry steps.

Among the adherent cells tested, 293T and HeLa cells showed high luciferase activity upon infection with both types of pseudotyped viruses, whereas NIH 3T3 cells yielded 10- to 100-fold-lower signals (Fig. 4). Similarly, the mouse T-cell lines BW5147, EL4, and YAC-1 displayed 100- to 1,000-fold-lower signals than did the human T-cell lines MT4 and Jurkat. Furthermore, luciferase expression efficiency was lower, by more than 1,000-fold, in mouse primary splenocytes than in human PBMCs. The relative sensitivity to infection of these cells was similar between the two pseudotyped viruses, although the efficiency of infection was approximately 10-fold higher in the HIV-1/VSV-G infection. Thus, these results again support a species-specific block in mouse cells subsequent to the entry step.

Reverse transcription of HIV-1 proceeds normally in mouse cells. We next evaluated the ability of mouse cells to support HIV-1 DNA synthesis. One day after infection, total DNA was harvested from various infected cells and subjected to quantitative PCR analyses. Both early (R-U5) and late (R-gag) reverse transcription products were specifically detected in DNA isolated from human and mouse cells exposed to both of the pseudotyped viruses, HIV-1/pJD-1 (Fig. 5A) and HIV-1/VSV-G (Fig. 5B). No R-U5 or R-gag products were detected when heat-inactivated (65°C, 1 h) viruses were infected, indicating that these products were not derived from the transfected HIV-1 DNA carryover. The copy number of R-U5, which reflects the efficiency of viral entry, was higher in mouse cells (NIH 3T3, BW5147, and splenocytes) than in human cells (HeLa, MT4, and PBMCs). The ratio of R-gag/R-U5 was calculated to evaluate the efficiency of the reverse transcription because R-U5 reflects the efficiency of entry (Fig. 5A and B, lower panels). No significant difference in the efficiency of reverse transcription was observed between mouse cells and human cells exposed to HIV-1/pJD-1 (Fig. 5A) and HIV-1/VSV-G (Fig. 5B). These results indicated that mouse cells supported reverse transcription at an efficiency similar to that of human cells.

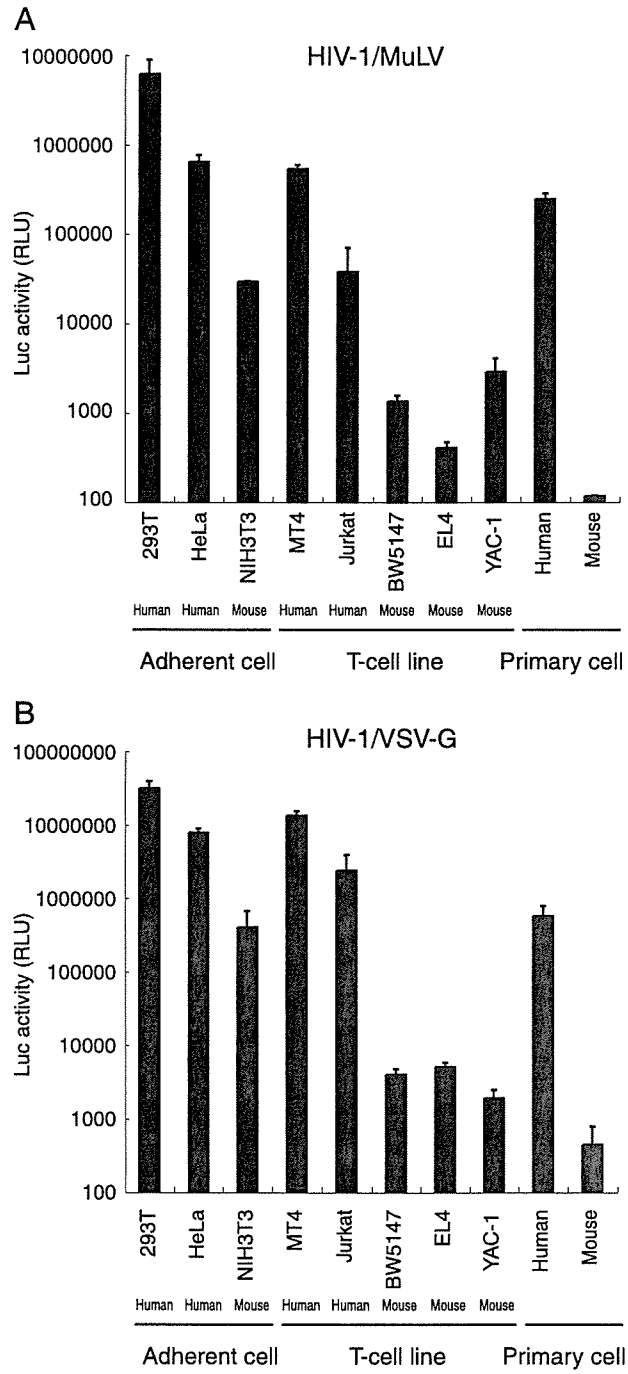

FIG. 4. Analysis of HIV-1 pseudotype virus replication in mouse cells. Human and murine cells were infected with equivalent doses of pNL43lucΔenv that was pseudotyped with either MuLV (A) or VSV-G (B) at 37°C for 6 h. After removal of the virus, cells were washed in growth medium. Luciferase activity was measured at 4 days postinfection, and normalized activities relative to the total protein quantity are shown. The data represent the means ± SEM of results from three wells. The data were reproduced in three independent experiments.

Nuclear import of the PIC is blocked in mouse cells. After completion of reverse transcription, the PIC crosses the

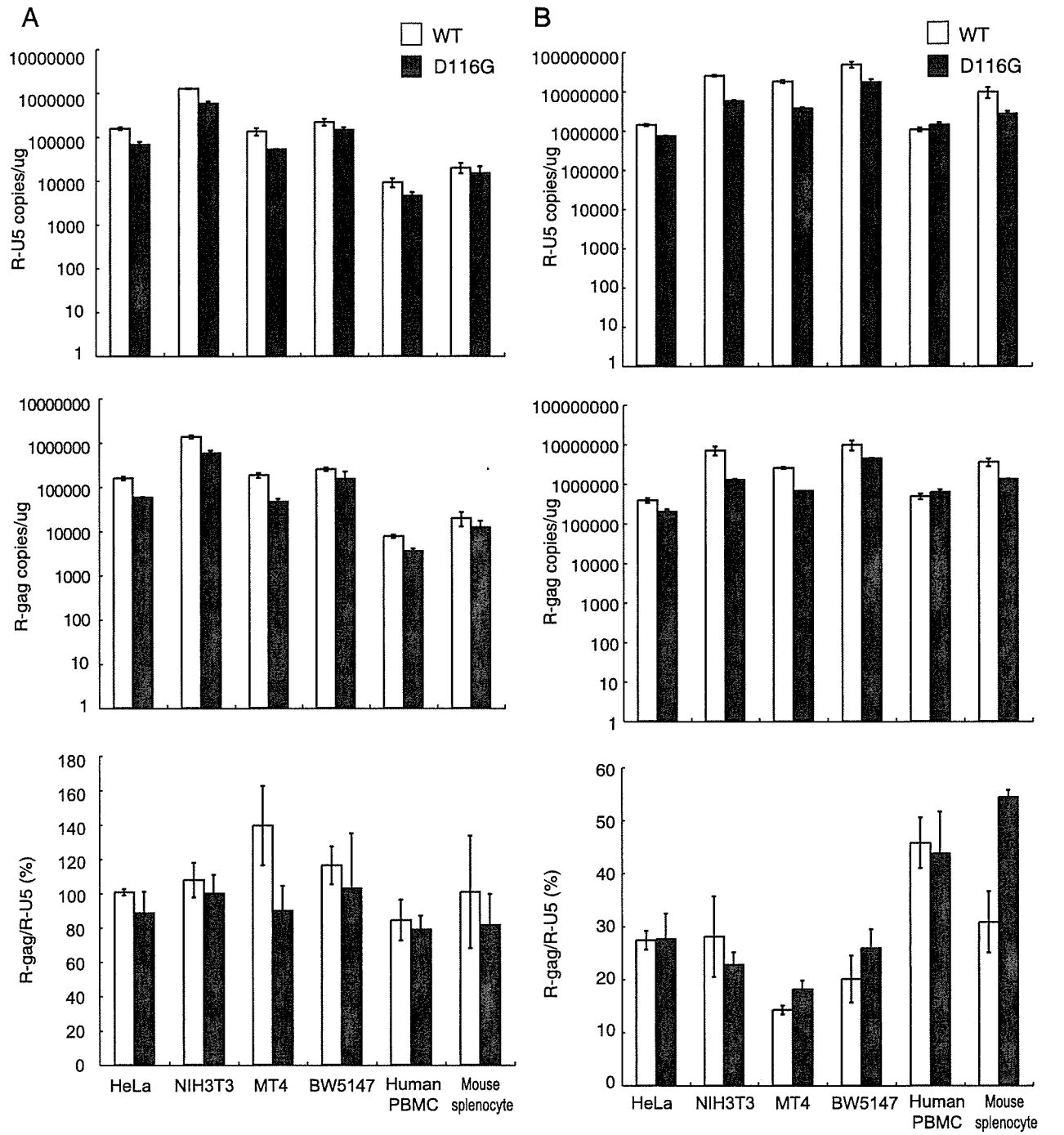

FIG. 5. The efficiency of the reverse transcription of HIV-1 in mouse cells. Human and murine cells were infected with equivalent doses of DNase-treated WT or integrase mutant (D116G) MuLV pseudotyped virus (A) or VSV-G pseudotyped virus (B). At 1 day postinfection, the cells were harvested, and the total DNA was extracted and subjected to quantitative real-time PCR analysis using primer pairs for R/U5 (upper panels) or R/gag (middle panels). The copy numbers of HIV-1 DNA per 1 μg β-actin are shown. The reverse transcription (RT) efficiency is calculated by dividing the late RT product (R-gag) by the early RT product (R-U5) (lower panel). The data represent the means ± SEM of results from three wells. The data were reproduced in three independent experiments.

nuclear membrane and enters the nucleus. Ligases within the nucleus then circularize the proviral DNA (2-LTR containing circular DNA) before its integration into the host chromosome (17, 57, 82). Although these 2-LTR circles are nonfunctional, they can serve as a measure of viral nuclear entry. To assess the efficiency of PIC transport into the nuclei of mouse cells, we estimated de novo-synthesized 2-LTR circular-form DNA by PCR using primer pairs that amplify sequences unique to this DNA form. The fragment corresponding to the 2-LTR circular junction was clearly

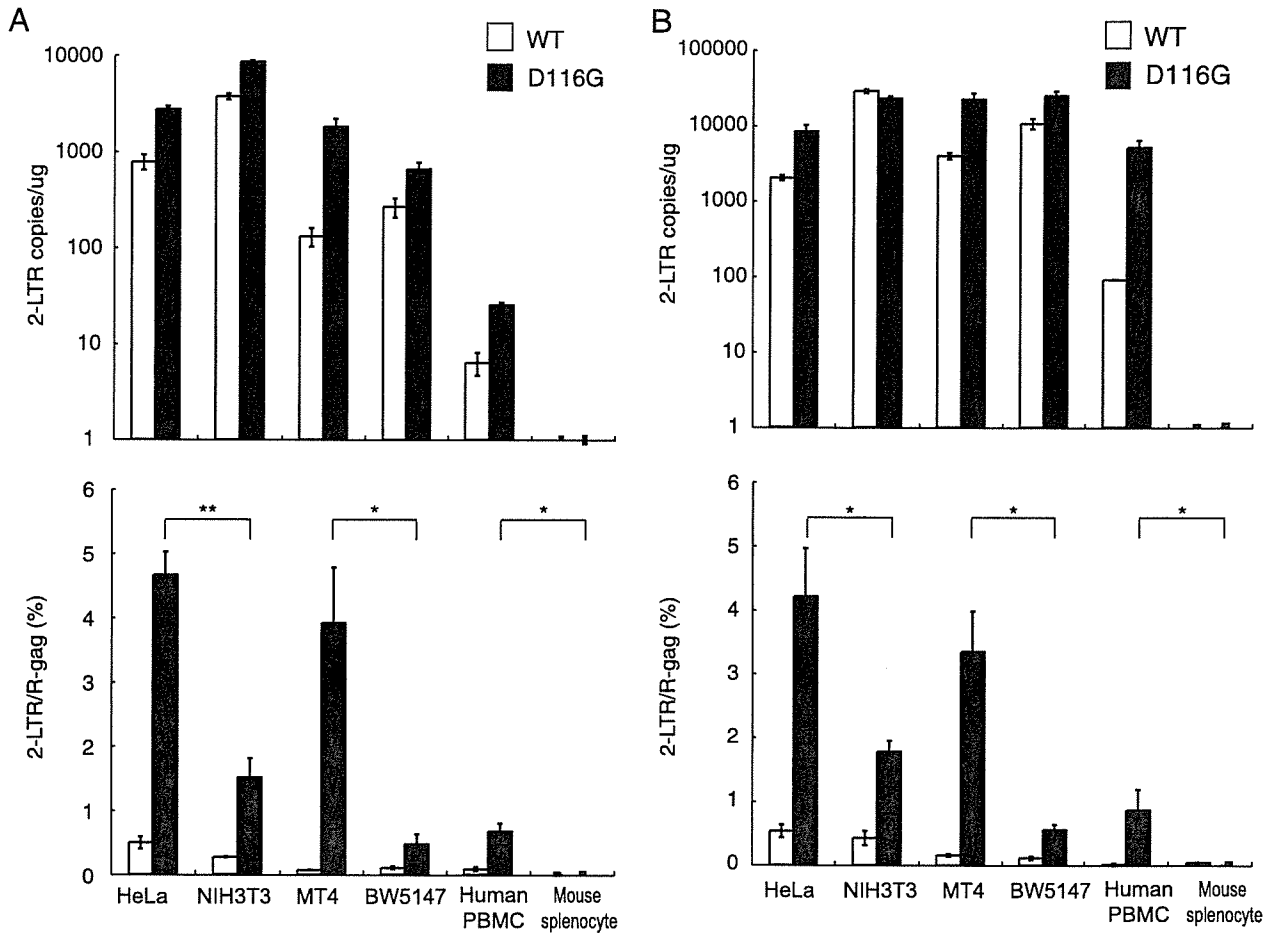

FIG. 6. Suppression of the 2-LTR circular form of DNA in mouse cells. Human and mouse cells were infected with equivalent doses of DNase-treated WT or integrase-mutant (D116G) MuLV pseudotype virus (A) or VSV-G pseudotype virus (B). The DNA from the infected cells was subjected to quantitative real-time PCR analysis using a primer pair specific for the 2-LTR circular form of the DNA (upper panels). The nuclear import efficiency was calculated by dividing the 2-LTR products by the late reverse transcription products (lower panels). The data represent the means ± SEM of results from three wells, and the data were reproduced in three independent experiments. *, $P < 0.05$; **, $P < 0.01$ (determined by Student's t test).

detected at 1 day postinfection in the DNA samples from HeLa, NIH 3T3, MT-4, BW5147, and human PBMCs infected with HIV-1/pJD-1 pseudotyped virus (Fig. 6A, upper panel). However, only a small amount of 2-LTR circle was detected in the mouse splenocytes. A similar tendency was observed in cells infected with the HIV-1/VSV-G pseudotyped virus (Fig. 6B, upper panel). The 2-LTR DNA in mouse cells was also measured at 2 and 4 days postinfection using both pseudotyped viruses and provided similar results (data not shown).

The ratio of 2-LTR/R-gag was calculated to evaluate the efficiency of nuclear import because the copy number of 2-LTR in the nucleus should be dependent on the amount of cytoplasmic R-gag, which represents the precursor of 2-LTR. The efficiency was very low and not significantly different between human and mouse when wild-type HIV-1 pseudovirus was infected (Fig. 6, lower panel). Because the nuclear concentration of 2-LTR is determined by the balance between accumulation of PIC by nuclear import and loss of PIC from the nucleoplasm by chromosome integration, we next used an integration-defective mutant, D116G, to examine only the efficiency of nuclear import. As shown in Fig. 6, the ratio was significantly lower in NIH 3T3 cells than in HeLa cells (33% or 43% of HeLa cells) and in BW5147 cells than in MT4 cells (12% or 17% of MT4 cells) when they were infected with HIV-1/pJD-1 or HIV-1/VSV-G, respectively (Fig. 6A and B, lower panels). We were unable to compare the efficiency of PIC import in human PBMCs and mouse splenocytes because the 2-LTR circle was not detected in mouse splenocytes. These results suggested that the nuclear import of the PIC is blocked in mouse cells, especially in splenocytes.

A block in the nuclear localization of the PIC is caused by a defect in IN nuclear localization. As Vpr and IN play important roles in importing the PIC into the nucleus, we hypothesized that Vpr and/or IN is nonfunctional in mouse cells due to the inability to utilize the cellular factors necessary for trafficking to the nucleus. To directly examine the karyophilic properties of HIV-1 IN in mouse cells, we generated an expression vector with HIV-1 IN in which the N terminus was fused to EGFP (GFP-IN). Since it was reported that β-galactosidase fusion to the C terminus of IN could not be located in

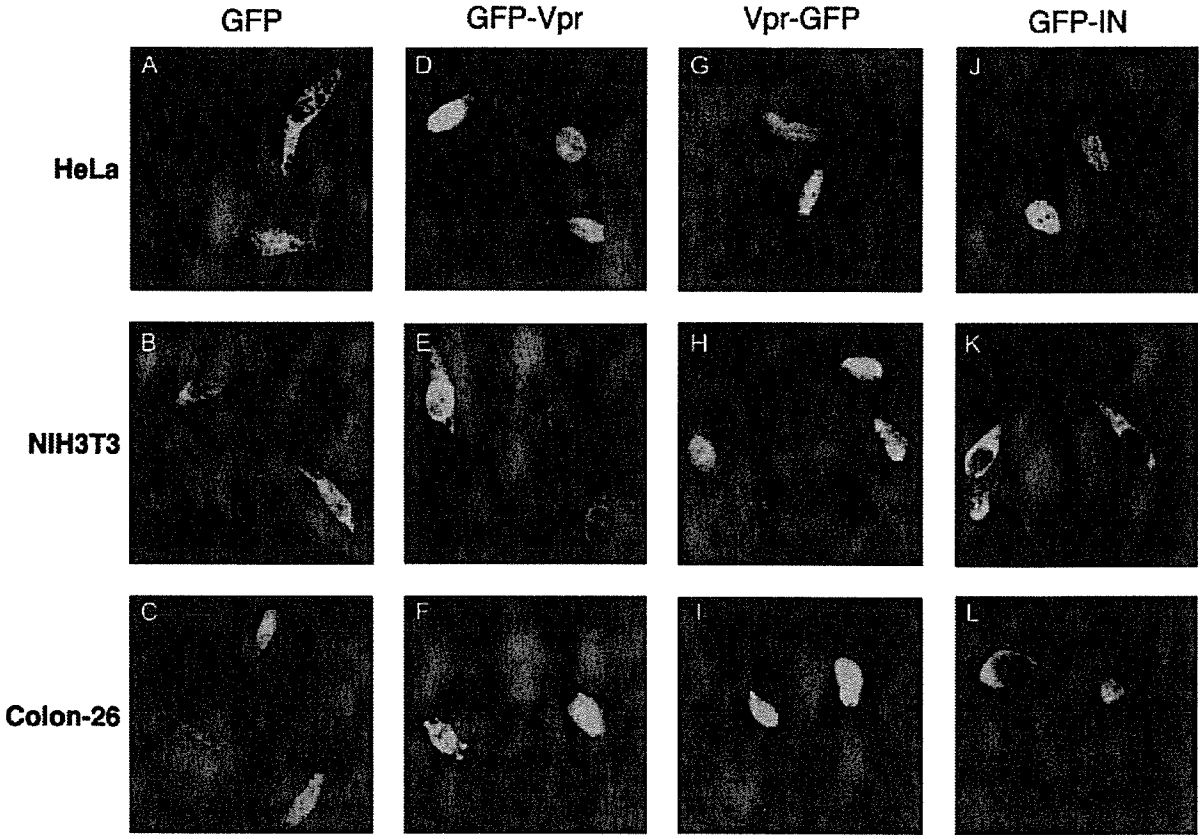

FIG. 7. Inhibition of IN-dependent GFP nuclear import in mouse cells. HeLa (A, D, G, and J), NIH 3T3 (B, E, H, and K), and Colon-26 cells (C, F, I, and L) were transfected with plasmids expressing GFP only (A, B, and C), GFP fused to the HIV-1 Vpr N terminus (GFP-Vpr) (D, E, and F), GFP fused to the HIV-1 Vpr C terminus (Vpr-GFP) (G, H, and I), and GFP fused to HIV-1 IN (J, K, and L) using Lipofectamine 2000. At 24 h posttransfection, the cells were fixed and visualized by confocal fluorescence microscopy. Note that the nuclear localization of GFP-IN is inhibited in mouse cells (K and L).

the nucleus (44), we did not examine the C terminus fusion construct (IN-GFP). We also generated HIV-1 Vpr expression vectors in which the N or C terminus was fused to EGFP (GFP-Vpr and Vpr-GFP, respectively). At 24 h postinfection, HeLa, NIH 3T3, and Colon-26 cells were transfected with the GFP fusion vectors, and the subcellular localization of IN or Vpr was examined with a confocal microscope. We used Colon-26 cells (Fv-1^n) in addition to NIH 3T3 cells (Fv-1^b) because Fv-1 may exert its antiretroviral effect at a postentry step, after reverse transcription and prior to integration (38, 79). Colon-26 cells and NIH 3T3 cells showed similar levels of luciferase activity upon infection with both types of pseudotyped viruses. Control GFP without IN or Vpr was distributed uniformly throughout both the cytoplasm and the nuclei in all cells examined (Fig. 7A to C). GFP-Vpr, on the other hand, accumulated almost exclusively in the nuclei of HeLa (Fig. 7D), NIH 3T3 (Fig. 7E), and Colon-26 (Fig. 7F) cells, although low levels of nuclear membrane association were also observed in NIH 3T3 cells (Fig. 7E). Vpr-GFP also accumulated almost exclusively in the nuclei of HeLa (Fig. 7G), NIH 3T3 (Fig. 7H), and Colon-26 (Fig. 7I) cells. These results indicated that HIV-1 Vpr has strong karyophilic properties and that, even in mouse cells, it can be transported across the nuclear membrane. In contrast, although GFP-IN accumulated almost exclusively in the nuclei of HeLa cells (Fig. 7J), GFP-IN was localized only in the cytoplasm of NIH 3T3 (Fig. 7K) and Colon-26 (Fig. 7L) cells. Thus, our results demonstrate that IN-mediated nuclear transport of HIV-1 PIC is impaired in mouse cells of both Fv-1 genotypes.

Addition of the SV40 NLS to the C terminus of HIV-1 integrase enhances viral infectivity in mouse cells. To analyze the role of IN in nuclear localization of HIV-1, we constructed an HIV-1 pNL43lucΔenv vector with the SV40 NLS at the C terminus of IN (IN-NLS), and pseudotyped virus was generated by cotransfection of 293T cells with the pNL43lucΔenv wild type or IN-NLS vector and VSV-G expression vector. Luciferase activity in the cell lysate of 293T cells transfected with IN-NLS was increased 2.5-fold compared to that transfected with wild-type virus (Fig. 8A). To verify that the gag-pol polyprotein processing was completed in IN-NLS virus particles, we performed Western blot analysis using an AIDS patient serum. No difference of the viral components was observed between parental WT and IN-NLS viruses (Fig. 8B). The content of p24 protein of the IN-NLS was also shown to be normal using a specific monoclonal antibody (data not shown). These results showed that addition of NLS to IN significantly activates viral replication.

Then we tested the susceptibility of HeLa, NIH 3T3, BW5147, and MT4 cells to IN-NLS infection. Addition of the

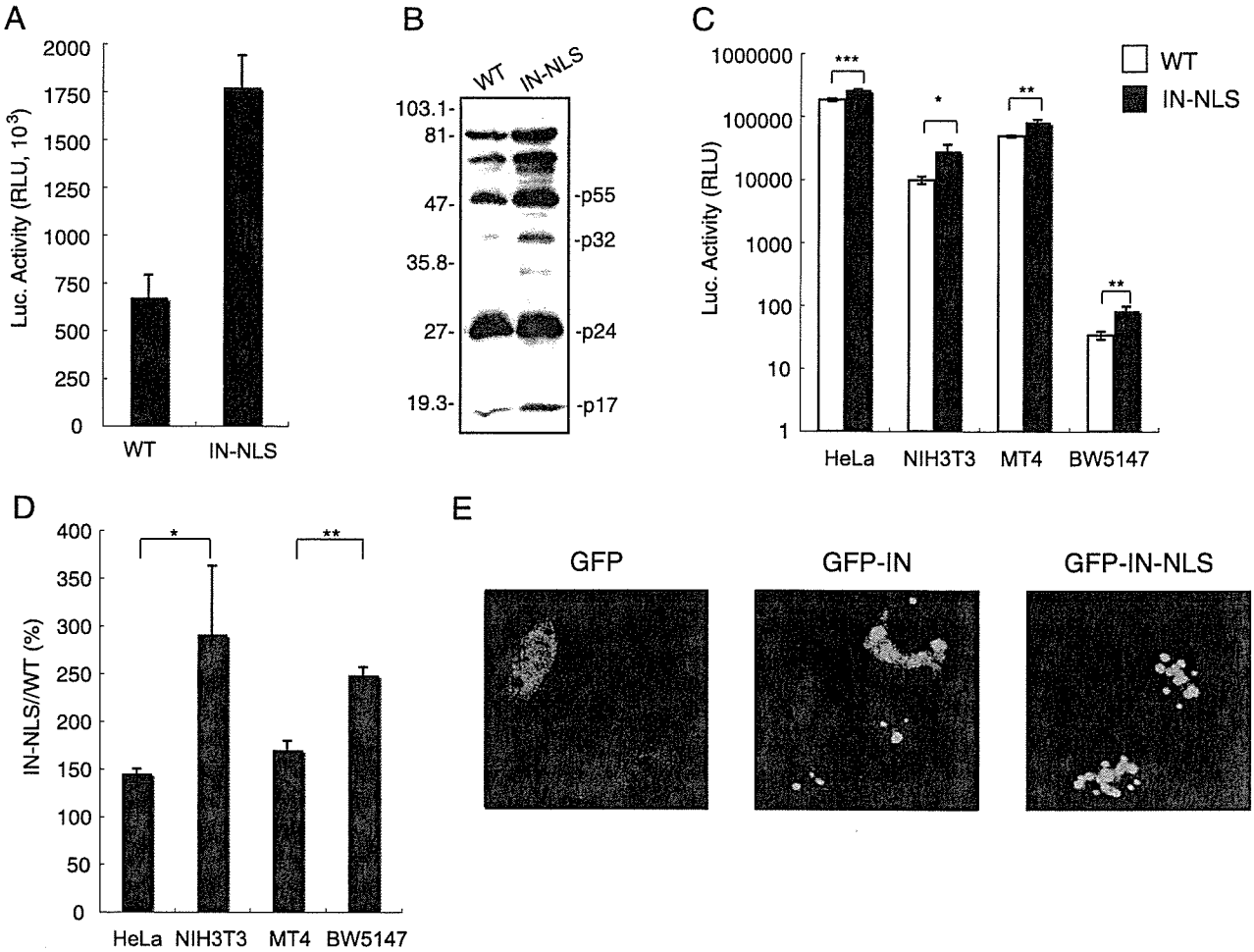

FIG. 8. Enhancement of viral infectivity to mouse cells by the addition of SV40 NLS to the C terminus of IN. (A) Luciferase activity in an HIV-1 pNL43lucΔenv vector (WT) or pNL43lucΔenv vector carrying an SV40 NLS-ligated IN (IN-NLS)-transfected 293T cells were measured at 2 days posttransfection. The data were reproduced in 10 independent experiments. (B) Virus particles were collected at 48 h posttransfection and resuspended in PBS. The viral pellets were hearted at 90°C for 10 min in the presence of sample buffer (62.5 mM Tris-HCl, pH 6.8, 10% glycerol, 2% SDS, 5% 2-mercaptoethanol, 0.005% bromophenol blue). Then viral proteins were electrophoresed on a 12% SDS–polyacrylamide gel. Viral proteins were detected with AIDS patient serum. Positions of the major viral proteins are indicated together with molecular weight markers. (C) Human and mouse cells were infected with equivalent amounts of WT (□) or IN-NLS (■) virus at 37°C for 6 h, and then the virus was removed. The luciferase activity was measured 4 days after infection, and the activity was normalized relative to the total amount of protein. Means ± SEM are shown. (D) Relative Luc activities of IN-NLS virus-infected cells compared to WT virus-infected cells were calculated using the data shown in panel C. Means ± SEM are shown. (E) NIH 3T3 cells transfected with a plasmid expressing GFP, GFP-IN, or GFP-IN-NLS fusion protein were analyzed by confocal microscopy. At 24 h posttransfection, cells were fixed and GFP was detected by a confocal fluorescent microscope. *, $P < 0.05$; **, $P < 0.01$; ***, $P < 0.001$ (by Student's t test).

SV40 NLS to the C terminus of IN significantly enhanced viral infectivity in all cell lines used (Fig. 8C). As the NLS fusion at the C terminus of IN disrupted the *vif* gene, we did not analyze the infectivity to human PBMC, which was nonpermissive to *vif*-deficient virus (24, 69). Interestingly, the effect of the NLS on viral infection was significantly stronger in mouse cells than in human cells (Fig. 8D).

We also analyzed the karyophilic property of GFP-IN-NLS in which EGFP was fused to the N terminus and the SV40 NLS at the C terminus of IN. GFP-IN-NLS accumulated almost exclusively in the nucleus of NIH 3T3 cells, in contrast to GFP-IN (Fig. 8E). These results indicate that the addition of functional NLS to IN compensates the functional defects of IN in mouse cells.

DISCUSSION

HIV-1 replication in rodent cells is blocked at multiple steps, including viral entry, transcription, nuclear export of the mRNA, assembly, and budding (77). In this study, we demonstrated that an additional host range barrier is present in mouse cells at the PIC nuclear transport step. We suggest that this restriction is caused by the dysfunction of the HIV-1 IN-dependent PIC import system.

We found that the ratio of the 2-LTR circular product to the late reverse transcription product (R-gag), which are produced in the nucleus and cytoplasm, respectively, was decreased in mouse splenocytes relative to human PBMCs after infection with both HIV-1/MuLV and HIV-1/VSV-G pseudotyped vi-

ruses (Fig. 6, lower panels). This indicates a reduction in nuclear import of the PIC. The efficiency of nuclear transfer of the viral PIC was recently reported to be reduced in mouse T cells relative to human T cell lines, but not in NIH 3T3 cells (7). These results are consistent with ours, although we cannot explain their lack of reduction in the NIH 3T3 cells. Our system using the IN mutant virus is probably more sensitive in detecting the defect.

We showed that the infection efficiency, as determined by luciferase activity, was 10 to 100, 100 to 1,000, and >1.000 times lower than in human cells in mouse adherent cells, T cell lines, and primary cells, respectively (Fig. 4). As the PIC nuclear import reduction in mouse cells was at most 60 to 90% compared to human cells (Fig. 6), it is clear that other barriers are also involved in the HIV-1 replication restriction in mouse cells. In this regard, we showed that the 2-LTR/R-gag ratio following infection with WT HIV-1 was similar between HeLa and NIH 3T3 cells and between MT4 and BW5147 cells, in contrast to our observations with the IN-deficient mutant virus (Fig. 6, lower panels). These results are explainable if the R-gag products integrate rapidly into the host chromosome in human cells compared to mouse cells, assuming that a constant proportion of free R-gag products is converted into the 2-LTR form. Thus, integration of the R-gag products into the host chromosome may also be inhibited in mouse cells. In accordance with this idea, we demonstrated that the integration frequency of HIV-1 was greatly reduced upon infection with WT HIV-1 in mouse cells transgenic for the huCD4/CXCR4 genes.

There are two formal explanations for the inability of the mouse cells to support HIV-1 PIC nuclear import. One is the absence of a required human-specific factor, and the other is the presence of an inhibitory factor(s) in mouse cells. However, because mouse-human cell fusions allow viral replication, mouse cells most likely do not have such an inhibitory factor and are rather devoid of a critical factor for the import of the HIV-1 PIC (52).

Although the mechanisms of PIC nuclear import have not been elucidated completely, NLSs are present in three viral proteins (MA, Vpr, and IN) as well as in a central DNA flap produced during reverse transcription that also contributes to the successful nuclear targeting of the PIC (59, 64, 71). Although their respective contributions remain controversial and unclear, it has been clearly shown that both Vpr and IN are karyophilic and rapidly accumulate in the nuclei of infected cells (6, 16, 19, 20, 25, 32, 48, 63, 66, 68). Meanwhile, localization of MA to the nucleus is not well established (14, 23). In this report, we demonstrated that GFP-fused IN remained in the cytoplasm of NIH 3T3 cells, in contrast to its accumulation in the nuclei of HeLa cells. On the other hand, when GFP-fused Vprs were examined, they localized to the nuclei of both NIH 3T3 and HeLa cells. The nuclear distribution of GFP-IN, but not GFP-fused Vpr, was also inhibited in the Colon-26 mouse cell line. These observations indicate that Vpr can be imported into the nucleus using separate pathways. IN, on the other hand, cannot be imported efficiently into the nuclei of mouse cells, and this is probably due to the inability of IN to interact with mouse nuclear import system.

In support for this notion, we showed that nuclear import of IN was much more enhanced in mouse cells than in human cells when authentic SV40 NLS was added to IN (Fig. 8). Furthermore, the addition of this NLS to IN significantly enhanced the infectivity of HIV-1 pseudovirus to mouse cells. These results indicate that endogenous nuclear localization signals of IN are not fully functional in mouse cells.

In this context, it is known that the NLSs within HIV-1 IN are composed of basic amino acid-rich sequences that interact with importin β through the adapter importin (25). We previously showed, however, that mutational disruption of the suggested NLSs could not abolish the nuclear localization of a GFP-IN fusion protein (76). Recent studies have shown that nonclassical NLSs are necessary and sufficient to locate the viral PIC into the nuclei (12). Depienne et al. suggested that the in vitro nuclear import of IN does not require known cytosolic transport factors, including karyopherin β family proteins (18). Two proteins have recently been reported to mediate PIC import. The first is lens epithelium-derived growth factor (LEDGF/p75), a protein implicated in the regulation of gene expression and cellular stress responses. LEDGF interacts with HIV-1 IN in vitro and in living cells (50) and colocalizes with HIV-IN in the nuclei of human cells (15). The second is importin 7, a mildly hydrophobic protein belonging to the importin β superfamily. This protein is suggested to interact with basic proteins, such as IN, that bind viral nucleic acids (21). It is currently unclear which protein(s) is important in these processes and defective in mouse cells. Clearly, further work is necessary to identify the host cell factors that are associated with IN in human cells and defective in mouse cells.

Thus far, several host restriction factors are known to be involved in the suppression of HIV-1 replication in the early phase of its life cycle in mouse cells. Friend virus susceptibility factor-1 (Fv-1) is involved in the restriction of specific mouse cell genotypes to MuLV (10, 28). The Fv-1 targets the MuLV capsid and stops the nuclear import of the PIC (8, 39). However, recent reports have noted that there is no correlation between HIV-1 susceptibility and cellular Fv-1 genotype (7, 31). Tripartite motif 5 α (TRIM5α), encoded by the gene *Lv-1*, is another restriction factor (72). TRIM5α inhibits viral replication in rhesus macaque cells at a step after entry but before the reverse transcription of HIV-1 by targeting the viral capsid protein (60). Thus, both Fv-1 and TRIM5α function in processes other than the transport of PIC into the nucleus.

In conclusion, we have demonstrated that PIC nuclear import is blocked in mouse cells and that dysfunctional IN is at least partially responsible for the barrier. Further characterization and identification of factors that are involved in PIC nuclear import should provide new insight into the molecular mechanisms of the PIC import step and clues to the development of new therapeutics. Furthermore, identification of the factors responsible for this step will assist in our generation of transgenic small animal models that are permissive to HIV-1 infection.

ACKNOWLEDGMENTS

We thank Takao Masuda (Tokyo Dental and Medical University) for providing pNL43lucΔenv and an amphotropic Moloney MuLV envelope expression vector (pJD-1) as well as for critical discussions. We also thank Yoshio Koyanagi (Kyoto University) for providing the 2-LTR plasmid and the AIDS patient serum and for important technical advice. We also thank Yoshio Inagaki (Tokyo Medical and Dental University) for providing the AIDS patient serum. We are grateful

to Luigi Naldini (San Raffaele Telethon Institute for Gene Therapy) and Kenzaburo Tani (Kyushu University) for providing the VSV-G envelope-expressing plasmid (pMD-G).

This work was supported by Grants-in-Aid from the Japan Human Sciences Foundation.

REFERENCES

1. **Adachi, A., H. E. Gendelman, S. Koenig, T. Folks, R. Willey, A. Rabson, and M. A. Martin.** 1986. Production of acquired immunodeficiency syndrome-associated retrovirus in human and nonhuman cells transfected with an infectious molecular clone. J. Virol. **59:**284–291.
2. **Aiken, C.** 1997. Pseudotyping human immunodeficiency virus type 1 (HIV-1) by the glycoprotein of vesicular stomatitis virus targets HIV-1 entry to an endocytic pathway and suppresses both the requirement for Nef and the sensitivity to cyclosporin A. J. Virol. **71:**5871–5877.
3. **Alonso, A., T. P. Cujec, and B. M. Peterlin.** 1994. Effects of human chromosome 12 on interactions between Tat and TAR of human immunodeficiency virus type 1. J. Virol. **68:**6505–6513.
4. **Alonso, A., D. Derse, and B. M. Peterlin.** 1992. Human chromosome 12 is required for optimal interactions between Tat and TAR of human immunodeficiency virus type 1 in rodent cells. J. Virol. **66:**4617–4621.
5. **Bai, Y., Y. Soda, K. Izawa, T. Tanabe, X. Kang, A. Tojo, H. Hoshino, H. Miyoshi, S. Asano, and K. Tani.** 2003. Effective transduction and stable transgene expression in human blood cells by a third-generation lentiviral vector. Gene Ther. **10:**1446–1457.
6. **Balliet, J. W., D. L. Kolson, G. Eiger, F. M. Kim, K. A. McGann, A. Srinivasan, and R. Collman.** 1994. Distinct effects in primary macrophages and lymphocytes of the human immunodeficiency virus type 1 accessory genes vpr, vpu, and nef: mutational analysis of a primary HIV-1 isolate. Virology **200:**623–631.
7. **Baumann, J. G., D. Unutmaz, M. D. Miller, S. K. Breun, S. M. Grill, J. Mirro, D. R. Littman, A. Rein, and V. N. KewalRamani.** 2004. Murine T cells potently restrict human immunodeficiency virus infection. J. Virol. **78:**12537–12547.
8. **Benit, L., N. De Parseval, J. F. Casella, I. Callebaut, A. Cordonnier, and T. Heidmann.** 1997. Cloning of a new murine endogenous retrovirus, MuERV-L, with strong similarity to the human HERV-L element and with a gag coding sequence closely related to the Fv1 restriction gene. J. Virol. **71:**5652–5657.
9. **Berson, J. F., D. Long, B. J. Doranz, J. Rucker, F. R. Jirik, and R. W. Doms.** 1996. A seven-transmembrane domain receptor involved in fusion and entry of T-cell-tropic human immunodeficiency virus type 1 strains. J. Virol. **70:**6288–6295.
10. **Best, S., P. Le Tissier, G. Towers, and J. P. Stoye.** 1996. Positional cloning of the mouse retrovirus restriction gene Fv1. Nature **382:**826–829.
11. **Bieniasz, P. D., and B. R. Cullen.** 2000. Multiple blocks to human immunodeficiency virus type 1 replication in rodent cells. J. Virol. **74:**9868–9877.
12. **Bouyac-Bertoia, M., J. D. Dvorin, R. A. Fouchier, Y. Jenkins, B. E. Meyer, L. I. Wu, M. Emerman, and M. H. Malim.** 2001. HIV-1 infection requires a functional integrase NLS. Mol. Cell **7:**1025–1035.
13. **Browning, J., J. W. Horner, M. Pettoello-Mantovani, C. Raker, S. Yurasov, R. A. DePinho, and H. Goldstein.** 1997. Mice transgenic for human CD4 and CCR5 are susceptible to HIV infection. Proc. Natl. Acad. Sci. USA **94:**14637–14641.
14. **Bukrinsky, M., K. Manogue, and A. Cerami.** 1995. HIV results in the frame. Other approaches. Nature **375:**195–196. (Author's reply, **375:**198.)
15. **Cherepanov, P., G. Maertens, P. Proost, B. Devreese, J. Van Beeumen, Y. Engelborghs, E. De Clercq, and Z. Debyser.** 2003. HIV-1 integrase forms stable tetramers and associates with LEDGF/p75 protein in human cells. J. Biol. Chem. **278:**372–381.
16. **Connor, R. I., B. K. Chen, S. Choe, and N. R. Landau.** 1995. Vpr is required for efficient replication of human immunodeficiency virus type-1 in mononuclear phagocytes. Virology **206:**935–944.
17. **Cullen, B. R.** 2001. Journey to the center of the cell. Cell **105:**697–700.
18. **Depienne, C., A. Mousnier, H. Leh, E. Le Rouzic, D. Dormont, S. Benichou, and C. Dargemont.** 2001. Characterization of the nuclear import pathway for HIV-1 integrase. J. Biol. Chem. **276:**18102–18107.
19. **Depienne, C., P. Roques, C. Creminon, L. Fritsch, R. Casseron, D. Dormont, C. Dargemont, and S. Benichou.** 2000. Cellular distribution and karyophilic properties of matrix, integrase, and Vpr proteins from the human and simian immunodeficiency viruses. Exp. Cell Res. **260:**387–395.
20. **Farnet, C. M., B. Wang, J. R. Lipford, and F. D. Bushman.** 1996. Differential inhibition of HIV-1 preintegration complexes and purified integrase protein by small molecules. Proc. Natl. Acad. Sci. USA **93:**9742–9747.
21. **Fassati, A., D. Gorlich, I. Harrison, L. Zaytseva, and J. M. Mingot.** 2003. Nuclear import of HIV-1 intracellular reverse transcription complexes is mediated by importin 7. EMBO J. **22:**3675–3685.
22. **Feng, Y., C. C. Broder, P. E. Kennedy, and E. A. Berger.** 1996. HIV-1 entry cofactor: functional cDNA cloning of a seven-transmembrane, G protein-coupled receptor. Science **272:**872–877.
23. **Fouchier, R. A., B. E. Meyer, J. H. Simon, U. Fischer, and M. H. Malim.** 1997. HIV-1 infection of non-dividing cells: evidence that the amino-terminal basic region of the viral matrix protein is important for Gag processing but not for post-entry nuclear import. EMBO J. **16:**4531–4539.
24. **Gabuzda, D. H., H. Li, K. Lawrence, B. S. Vasir, K. Crawford, and E. Langhoff.** 1994. Essential role of vif in establishing productive HIV-1 infection in peripheral blood T lymphocytes and monocyte/macrophages. J. Acquir. Immune Defic. Syndr. **7:**908–915.
25. **Gallay, P., T. Hope, D. Chin, and D. Trono.** 1997. HIV-1 infection of nondividing cells through the recognition of integrase by the importin/karyopherin pathway. Proc. Natl. Acad. Sci. USA **94:**9825–9830.
26. **Garber, M. E., and K. A. Jones.** 1999. HIV-1 Tat: coping with negative elongation factors. Curr. Opin. Immunol. **11:**460–465.
27. **Garber, M. E., P. Wei, V. N. KewalRamani, T. P. Mayall, C. H. Herrmann, A. P. Rice, D. R. Littman, and K. A. Jones.** 1998. The interaction between HIV-1 Tat and human cyclin T1 requires zinc and a critical cysteine residue that is not conserved in the murine CycT1 protein. Genes Dev. **12:**3512–3527.
28. **Goff, S. P.** 1996. Operating under a Gag order: a block against incoming virus by the Fv1 gene. Cell **86:**691–693.
29. **Habu, K., J. Nakayama-Yamada, M. Asano, S. Saijo, K. Itagaki, R. Horai, H. Yamamoto, T. Sekiguchi, T. Nosaka, M. Hatanaka, and Y. Iwakura.** 1999. The human T cell leukemia virus type I-tax gene is responsible for the development of both inflammatory polyarthropathy resembling rheumatoid arthritis and noninflammatory ankylotic arthropathy in transgenic mice. J. Immunol. **162:**2956–2963.
30. **Hart, C. E., C. Y. Ou, J. C. Galphin, J. Moore, L. T. Bacheler, J. J. Wasmuth, S. R. Petteway, Jr., and G. Schochetman.** 1989. Human chromosome 12 is required for elevated HIV-1 expression in human-hamster hybrid cells. Science **246:**488–491.
31. **Hatziioannou, T., S. Cowan, and P. D. Bieniasz.** 2004. Capsid-dependent and -independent postentry restriction of primate lentivirus tropism in rodent cells. J. Virol. **78:**1006–1011.
32. **Heinzinger, N. K., M. I. Bukinsky, S. A. Haggerty, A. M. Ragland, V. Kewalramani, M. A. Lee, H. E. Gendelman, L. Ratner, M. Stevenson, and M. Emerman.** 1994. The Vpr protein of human immunodeficiency virus type 1 influences nuclear localization of viral nucleic acids in nondividing host cells. Proc. Natl. Acad. Sci. USA **91:**7311–7315.
33. **Ho, S. N., H. D. Hunt, R. M. Horton, J. K. Pullen, and L. R. Pease.** 1989. Site-directed mutagenesis by overlap extension using the polymerase chain reaction. Gene **77:**51–59.
34. **Hogan, B., E. Constantini, and E. Lacey.** 1994. Manipulating the mouse embryo: a laboratory manual, 2nd ed. Cold Spring Harbor Laboratory Press, Cold Spring Harbor, NY.
35. **Isegawa, Y., J. Sheng, Y. Sokawa, K. Yamanishi, O. Nakagomi, and S. Ueda.** 1992. Selective amplification of cDNA sequence from total RNA by cassette-ligation mediated polymerase chain reaction (PCR): application to sequencing 6.5 kb genome segment of hantavirus strain B-1. Mol. Cell Probes **6:**467–475.
36. **Iwakura, Y., T. Shioda, M. Tosu, E. Yoshida, M. Hayashi, T. Nagata, and H. Shibuta.** 1992. The induction of cataracts by HIV-1 in transgenic mice. AIDS **6:**1069–1075.
37. **Jackson, J. B., K. L. MacDonald, J. Cadwell, C. Sullivan, W. E. Kline, M. Hanson, K. J. Sannerud, S. L. Stramer, N. J. Fildes, S. Y. Kwok, et al.** 1990. Absence of HIV infection in blood donors with indeterminate western blot tests for antibody to HIV-1. N. Engl. J. Med. **322:**217–222.
38. **Jolicoeur, P., and D. Baltimore.** 1976. Effect of Fv-1 gene product on proviral DNA formation and integration in cells infected with murine leukemia viruses. Proc. Natl. Acad. Sci. USA **73:**2236–2240.
39. **Jolicoeur, P., and E. Rassart.** 1980. Effect of Fv-1 gene product on synthesis of linear and supercoiled viral DNA in cells infected with murine leukemia virus. J. Virol. **33:**183–195.
40. **Keppler, O. T., W. Yonemoto, F. J. Welte, K. S. Patton, D. Iacovides, R. E. Atchison, T. Ngo, D. L. Hirschberg, R. F. Speck, and M. A. Goldsmith.** 2001. Susceptibility of rat-derived cells to replication by human immunodeficiency virus type 1. J. Virol. **75:**8063–8073.
41. **Klatzmann, D., E. Champagne, S. Chamaret, J. Gruest, D. Guetard, T. Hercend, J. C. Gluckman, and L. Montagnier.** 1984. T-lymphocyte T4 molecule behaves as the receptor for human retrovirus LAV. Nature **312:**767–768.
42. **Koito, A., Y. Kameyama, C. Cheng-Mayer, and S. Matsushita.** 2003. Susceptibility of mink (Mustera vision)-derived cells to replication by human immunodeficiency virus type 1. J. Virol. **77:**5109–5117.
43. **Koito, A., H. Shigekane, and S. Matsushita.** 2003. Ability of small animal cells to support the postintegration phase of human immunodeficiency virus type-1 replication. Virology **305:**181–191.
44. **Kukolj, G., K. S. Jones, and A. M. Skalka.** 1997. Subcellular localization of avian sarcoma virus and human immunodeficiency virus type 1 integrases. J. Virol. **71:**843–847.
45. **Kwok, S., D. E. Kellogg, N. McKinney, D. Spasic, L. Goda, C. Levenson, and J. J. Sninsky.** 1990. Effects of primer-template mismatches on the polymerase chain reaction: human immunodeficiency virus type 1 model studies. Nucleic Acids Res. **18:**999–1005.

46. **Landau, N. R., M. Warton, and D. R. Littman.** 1988. The envelope glycoprotein of the human immunodeficiency virus binds to the immunoglobulin-like domain of CD4. Nature **334**:159–162.
47. **Lores, P., V. Boucher, C. Mackay, M. Pla, H. Von Boehmer, J. Jami, F. Barre-Sinoussi, and J. C. Weill.** 1992. Expression of human CD4 in transgenic mice does not confer sensitivity to human immunodeficiency virus infection. AIDS Res. Hum. Retrovir. **8**:2063–2071.
48. **Lu, Y. L., P. Spearman, and L. Ratner.** 1993. Human immunodeficiency virus type 1 viral protein R localization in infected cells and virions. J. Virol. **67**:6542–6550.
49. **Maddon, P. J., A. G. Dalgleish, J. S. McDougal, P. R. Clapham, R. A. Weiss, and R. Axel.** 1986. The T4 gene encodes the AIDS virus receptor and is expressed in the immune system and the brain. Cell **47**:333–348.
50. **Maertens, G., P. Cherepanov, W. Pluymers, K. Busschots, E. De Clercq, Z. Debyser, and Y. Engelborghs.** 2003. LEDGF/p75 is essential for nuclear and chromosomal targeting of HIV-1 integrase in human cells. J. Biol. Chem. **278**:33528–33539.
51. **Mancebo, H. S., G. Lee, J. Flygare, J. Tomassini, P. Luu, Y. Zhu, J. Peng, C. Blau, D. Hazuda, D. Price, and O. Flores.** 1997. P-TEFb kinase is required for HIV Tat transcriptional activation in vivo and in vitro. Genes Dev. **11**:2633–2644.
52. **Mariani, R., B. A. Rasala, G. Rutter, K. Wiegers, S. M. Brandt, H. G. Krausslich, and N. R. Landau.** 2001. Mouse-human heterokaryons support efficient human immunodeficiency virus type 1 assembly. J. Virol. **75**:3141–3151.
53. **Mariani, R., G. Rutter, M. E. Harris, T. J. Hope, H. G. Krausslich, and N. R. Landau.** 2000. A block to human immunodeficiency virus type 1 assembly in murine cells. J. Virol. **74**:3859–3870.
54. **Masuda, T., V. Planelles, P. Krogstad, and I. S. Chen.** 1995. Genetic analysis of human immunodeficiency virus type 1 integrase and the U3 att site: unusual phenotype of mutants in the zinc finger-like domain. J. Virol. **69**: 6687–6696.
55. **Miller, D. G., and A. D. Miller.** 1994. A family of retroviruses that utilize related phosphate transporters for cell entry. J. Virol. **68**:8270–8276.
56. **Morikawa, Y., S. Hinata, H. Tomoda, T. Goto, M. Nakai, C. Aizawa, H. Tanaka, and S. Omura.** 1996. Complete inhibition of human immunodeficiency virus Gag myristoylation is necessary for inhibition of particle budding. J. Biol. Chem. **271**:2868–2873.
57. **Neil, S., F. Martin, Y. Ikeda, and M. Collins.** 2001. Postentry restriction to human immunodeficiency virus-based vector transduction in human monocytes. J. Virol. **75**:5448–5456.
58. **Newstein, M., E. J. Stanbridge, G. Casey, and P. R. Shank.** 1990. Human chromosome 12 encodes a species-specific factor which increases human immunodeficiency virus type 1 tat-mediated trans activation in rodent cells. J. Virol. **64**:4565–4567.
59. **Nisole, S., and A. Saib.** 2004. Early steps of retrovirus replicative cycle. Retrovirology **1**:9.
60. **Nisole, S., J. P. Stoye, and A. Saib.** 2005. TRIM family proteins: retroviral restriction and antiviral defence. Nat. Rev. Microbiol. **3**:799–808.
61. **Nomura, H., B. W. Nielsen, and K. Matsushima.** 1993. Molecular cloning of cDNAs encoding a LD78 receptor and putative leukocyte chemotactic peptide receptors. Int. Immunol. **5**:1239–1249.
62. **Ory, D. S., B. A. Neugeboren, and R. C. Mulligan.** 1996. A stable human-derived packaging cell line for production of high titer retrovirus/vesicular stomatitis virus G pseudotypes. Proc. Natl. Acad. Sci. USA **93**:11400–11406.
63. **Petit, C., O. Schwartz, and F. Mammano.** 2000. The karyophilic properties of human immunodeficiency virus type 1 integrase are not required for nuclear import of proviral DNA. J. Virol. **74**:7119–7126.
64. **Piller, S. C., L. Caly, and D. A. Jans.** 2003. Nuclear import of the pre-integration complex (PIC): the Achilles heel of HIV? Curr. Drug Targets **4**:409–429.
65. **Planelles, V., A. Haislip, E. S. Withers-Ward, S. A. Stewart, Y. Xie, N. P. Shah, and I. S. Chen.** 1995. A new reporter system for detection of retroviral infection. Gene Ther. **2**:369–376.
66. **Pluymers, W., P. Cherepanov, D. Schols, E. De Clercq, and Z. Debyser.** 1999. Nuclear localization of human immunodeficiency virus type 1 integrase expressed as a fusion protein with green fluorescent protein. Virology **258**:327–332.
67. **Pollard, V. W., and M. H. Malim.** 1998. The HIV-1 Rev protein. Annu. Rev. Microbiol. **52**:491–532.
68. **Popov, S., M. Rexach, G. Zybarth, N. Reiling, M. A. Lee, L. Ratner, C. M. Lane, M. S. Moore, G. Blobel, and M. Bukrinsky.** 1998. Viral protein R regulates nuclear import of the HIV-1 pre-integration complex. EMBO J. **17**:909–917.
69. **Sakai, H., R. Shibata, J. Sakuragi, S. Sakuragi, M. Kawamura, and A. Adachi.** 1993. Cell-dependent requirement of human immunodeficiency virus type 1 Vif protein for maturation of virus particles. J. Virol. **67**:1663–1666.
70. **Sawada, S., K. Gowrishankar, R. Kitamura, M. Suzuki, G. Suzuki, S. Tahara, and A. Koito.** 1998. Disturbed CD4+ T cell homeostasis and in vitro HIV-1 susceptibility in transgenic mice expressing T cell line-tropic HIV-1 receptors. J. Exp. Med. **187**:1439–1449.
71. **Sherman, M. P., and W. C. Greene.** 2002. Slipping through the door: HIV entry into the nucleus. Microbes Infect. **4**:67–73.
72. **Stremlau, M., C. M. Owens, M. J. Perron, M. Kiessling, P. Autissier, and J. Sodroski.** 2004. The cytoplasmic body component TRIM5alpha restricts HIV-1 infection in Old World monkeys. Nature **427**:848–853.
73. **Suzuki, Y., N. Misawa, C. Sato, H. Ebina, T. Masuda, N. Yamamoto, and Y. Koyanagi.** 2003. Quantitative analysis of human immunodeficiency virus type 1 DNA dynamics by real-time PCR: integration efficiency in stimulated and unstimulated peripheral blood mononuclear cells. Virus Genes **27**:177–188.
74. **Tanaka, J., H. Ozaki, J. Yasuda, R. Horai, Y. Tagawa, M. Asano, S. Saijo, M. Imai, K. Sekikawa, M. Kopf, and Y. Iwakura.** 2000. Lipopolysaccharide-induced HIV-1 expression in transgenic mice is mediated by tumor necrosis factor-alpha and interleukin-1, but not by interferon-gamma nor interleukin-6. AIDS **14**:1299–1307.
75. **Tsuruo, T., T. Yamori, K. Naganuma, S. Tsukagoshi, and Y. Sakurai.** 1983. Characterization of metastatic clones derived from a metastatic variant of mouse colon adenocarcinoma 26. Cancer Res. **43**:5437–5442.
76. **Tsurutani, N., M. Kubo, Y. Maeda, T. Ohashi, N. Yamamoto, M. Kannagi, and T. Masuda.** 2000. Identification of critical amino acid residues in human immunodeficiency virus type 1 IN required for efficient proviral DNA formation at steps prior to integration in dividing and nondividing cells. J. Virol. **74**:4795–4806.
77. **van Maanen, M., and R. E. Sutton.** 2003. Rodent models for HIV-1 infection and disease. Curr. HIV Res. **1**:121–130.
78. **Wei, P., M. E. Garber, S. M. Fang, W. H. Fischer, and K. A. Jones.** 1998. A novel CDK9-associated C-type cyclin interacts directly with HIV-1 Tat and mediates its high-affinity, loop-specific binding to TAR RNA. Cell **92**:451–462.
79. **Yang, W. K., J. O. Kiggans, D. M. Yang, C. Y. Ou, R. W. Tennant, A. Brown, and R. H. Bassin.** 1980. Synthesis and circularization of N- and B-tropic retroviral DNA Fv-1 permissive and restrictive mouse cells. Proc. Natl. Acad. Sci. USA **77**:2994–2998.
80. **Yasuda, J., T. Miyao, M. Kamata, Y. Aida, and Y. Iwakura.** 2001. T cell apoptosis causes peripheral T cell depletion in mice transgenic for the HIV-1 vpr gene. Virology **285**:181–192.
81. **Zack, J. A., S. J. Arrigo, S. R. Weitsman, A. S. Go, A. Haislip, and I. S. Chen.** 1990. HIV-1 entry into quiescent primary lymphocytes: molecular analysis reveals a labile, latent viral structure. Cell **61**:213–222.
82. **Zennou, V., C. Petit, D. Guetard, U. Nerhbass, L. Montagnier, and P. Charneau.** 2000. HIV-1 genome nuclear import is mediated by a central DNA flap. Cell **101**:173–185.
83. **Zheng, Y. H., H. F. Yu, and B. M. Peterlin.** 2003. Human p32 protein relieves a post-transcriptional block to HIV replication in murine cells. Nat. Cell Biol. **5**:611–618.